Calcolo (2014) 51:329–362
DOI 10.1007/s10092-013-0088-2

Shape preservation of scientific data through rational fractal splines

A. K. B. Chand · N. Vijender · M. A. Navascués

Received: 24 October 2012 / Accepted: 26 March 2013 / Published online: 22 May 2013
© Springer-Verlag Italia 2013

Abstract Fractal interpolation is a modern technique in approximation theory to fit and analyze scientific data. We develop a new class of $\mathcal{C}^1$- rational cubic fractal interpolation functions, where the associated iterated function system uses rational functions of the form $\frac{p_i(x)}{q_i(x)}$, where $p_i(x)$ and $q_i(x)$ are cubic polynomials involving two shape parameters. The rational cubic iterated function system scheme provides an additional freedom over the classical rational cubic interpolants due to the presence of the scaling factors and shape parameters. The classical rational cubic functions are obtained as a special case of the developed fractal interpolants. An upper bound of the uniform error of the rational cubic fractal interpolation function with an original function in $\mathcal{C}^2$ is deduced for the convergence results. The rational fractal scheme is computationally economical, very much local, moderately local or global depending on the scaling factors and shape parameters. Appropriate restrictions on the scaling factors and shape parameters give sufficient conditions for a shape preserving rational cubic fractal interpolation function so that it is monotonic, positive, and convex if the data set is monotonic, positive, and convex, respectively. A visual illustration of the shape preserving fractal curves is provided to support our theoretical results.

A. K. B. Chand (✉) · N. Vijender
Department of Mathematics, Indian Institute of Technology Madras, Chennai 600036, India
e-mail: chand@iitm.ac.in

N. Vijender
e-mail: vijendernallapu@gmail.com

M. A. Navascués
Departmento de Matemática Aplicada, Escuela de Ingeniería y Arquitectura,
Universidad de Zaragoza, C/ María de Luna 3, Zaragoza 50018, Spain
e-mail: manavas@unizar.es

Keywords Fractals · Iterated function systems · Fractal interpolation functions · Rational cubic fractal functions · Rational cubic interpolation · Monotonicity · Positivity · Convexity

Mathematics Subject Classification (2000) 28A80 · 41A20 · 65D10 · 41A25 · 65D05 · 65D07 · 26A48 · 26A51

1 Introduction

Mandelbrot [26] has revolutionized the applications of the fractal geometry in natural sciences and engineering. Fractals through their various forms cover pre-existing concepts from the pure mathematics to the most empirical aspects of engineering [11,13,21,40]. There exist several mathematical constructions of fractals that are classified as algebraic, analytic, and stochastic methods. All these methods describe different aspects of the complex structures of fractals that represent either the ideas of scientists or the data from natural, scientific, and engineering phenomena. Interpolation techniques play a very important role in data visualization. The classical interpolation techniques fit an elementary function to the given data in order to render a connected visualization of a sample. Such elementary functions often imbue the visualization with a degree of smoothness that may not be consistent with the nature of a prescribed data set. Fractals and fractal interpolation functions have been applied to prevent such inappropriate smoothing [27,39]. Utilizing the iterated function system (IFS) theory [2,3,22], some authors proposed the concept of a fractal interpolation function (FIF) such that it is the attractor of a specific IFS. In general, FIFs are fixed points of the Read–Bajraktarević operator, which are defined on suitable function spaces. Using fractal interpolation methodology, it is possible to construct interpolants with integer and non-integer dimensions. By imposing suitable conditions on the scaling factors, Barnsley and Harrington [4] introduced the construction of k-times differentiable FIFs, if up to kth order derivative values of the original function are known at the initial end point, but it is difficult to get all types of boundary conditions for fractal splines in this iterative construction. Fractal splines with general boundary conditions have recently been studied [6–8,28] in simpler ways.

Interpolation techniques play a very important role in obtaining solutions of various problems that arise in many areas of scientific computation such as computer graphics, computer aided design, information sciences, and data visualization. Usually, a designer provides the envelopes of a car body, ship hull, airplane fuselage, engine details of complex shape, etc. as a discrete set of points. To produce the body, one needs to describe these points as lying on a curve or a surface with a particular shape. Positivity, monotonicity, convexity are the fundamental and important shape properties. For instance, positive data arise in monthly rainfall amounts, levels of gas discharge in certain chemical reactions, progress of an irreversible process, resistance offered by an electric circuit, etc. The negative graphical display of these physical quantities is meaningless. Monotonicity is another very important feature of an interpolation data. Monotonicity preserving interpolants play important roles in various scientific problems. Approximation of couples and quasi couples in statistics [5], rate of dissemination of drug in blood [5], fuzzy logic [41], empirical option of pricing models in finance [23] are good examples of monotonic data. Convexity preserving interpolation plays a vital role in non-linear programming which arises in engineering and scientific applications such as design, optimal control, parameter estimation, and approximation of functions. Construction of shape preserving interpolation functions was initiated by Schweikert [35]. Fritsch and Carlson [14] and Fritsch and Butland [15] have developed piecewise cubic polynomials for monotonicity preserving interpolation. They made a modification in input derivatives in their interpolants if the derivatives contravene the necessary monotonicity conditions. By inserting an extra knot in each sub-interval, Schumaker [34] constructed a monotonicity preserving piecewise quadratic interpolant. Lamberti [25] used the cubic Hermite in parametric form to preserve the shape of planar functional data. The step lengths were used as tension parameters to the shape inherent to the data. The first order derivatives at the knots were estimated by a tridiagonal system of equations which assured $\mathcal{C}^2$ continuity at the knots. Some more shape preserving polynomial interpolating techniques were carried out by Passow and Roulier [17], Goodman and Unsworth [29] and Passow [30]. Since polynomial spline representation is unique for a given data, there is no freedom for a user to modify the curve, and hence it may not be suitable for interactive design problems. An alternative to the use of polynomials for shape preserving interpolation is the application of piecewise rational quadratic functions by Gregory and Delbourgo [18,19]. These shape preserving rational interpolants do not contain any shape parameter. But it is not possible to modify the curves generated by these schemes. By introducing a shape parameter in each sub-interval, Delbourgo and Gregory [10] developed a shape preserving rational cubic interpolant for local shape modification. Thus they settled a powerful tool to modify the shape of data according to the requirement in the form of shape parameter. Using this technique, huge number of shape preserving interpolants with shape parameters have been developed, see for instance ([20,31,32,37,38]; and references therein). Rational splines have vast applications in reverse engineering, and vectorization of object (CAD) [24]. Fuhr and Kallay [16] used a monotonic rational B-spline of degree one to preserve the shape of monotonic data.

Utilizing the fractal methodology, our group has introduced a novel approach to construct (i) monotonic rational quadratic FIFs (ii) shape preserving rational cubic fractal splines. In the present work, we introduce a class of $\mathcal{C}^1$-rational cubic fractal interpolants with two-families of shape parameters for representation of monotonic, positive, and convex data, and this includes the corresponding classical rational cubic interpolant [31] as a special case. Our rational fractal interpolant contains free parameters called the scaling factors in addition to the two families of shape parameters contained in its classical counterpart. Due to the implicit nature of FIFs, it is not possible to generate the shape preserving (monotonicity and convexity) rational cubic FIFs based on necessary conditions on the derivatives at knots. Therefore, sufficient conditions are derived through the restrictions on the scaling vector and shape parameters. Based on the Banach Fixed Point Theorem, the rational cubic fractal interpolant curve representation is unique for a given set of the scaling factors and shape parameters. In addition to the pleasant display, the developed fractal rational scheme provides an extra degree of freedom through the scaling vector over the classical rational interpolant to a user to play with the shape of a rational cubic fractal curve, and to modify it according to the need of application.

This paper is organized as follows: Preliminaries of FIFs via IFS theory are presented in Sect. 2. The general construction of a rational cubic FIF involving two families of shape parameters, their shape control analysis, and approximation properties are discussed in Sect. 3. Suitable conditions on the scaling factors and shape parameters are deduced to preserve the monotonicity, positivity, or convexity nature of a given data in Sect. 4, and these results are implemented in Sect. 5 to construct the desired shape preserving fractal interpolants.

2 Fractal interpolation functions

The basics of IFS theory is discussed in Sect. 2.1, and the construction of a FIF from an IFS is given in Sect. 2.2.

2.1 IFS theory

Let $(\mathcal{X}, d)$ be a complete metric space, and $\mathcal{H}(\mathcal{X})$ be the set of all nonempty compact subsets of $\mathcal{X}$. Then $\mathcal{H}(\mathcal{X})$ is a complete metric space with respect to the Hausdorff metric h, where h is defined as $\mathsf{h}(A, B) = \max\{d(A, B), d(B, A)\}$, and

$$d(A, B) = \max_{x\in A}\min_{y\in B}\ d(x, y).$$

Let $\vartheta_i : \mathcal{X} \to \mathcal{X}$ be continuous functions for $i = 1, 2, \ldots, n-1$. The set $\mathcal{I} = \{\mathcal{X}; \vartheta_i, i = 1, 2, \ldots, n-1\}$ is called an IFS. An IFS $\mathcal{I}$ is called *hyperbolic* if

$$\frac{d(\vartheta_i(x), \vartheta_i(y))}{d(x, y)} \le |c_i| < 1, \quad \forall\, x \neq y \in \mathcal{X}.$$

For any $A \in \mathcal{H}(\mathcal{X})$, we define the set valued Hutchinson function V on $\mathcal{H}(\mathcal{X})$ as

$$V(A) = \bigcup_{i\in\{1,2,\ldots,n-1\}} \vartheta_i(A).$$

If IFS $\mathcal{I}$ is *hyperbolic,* then it is easy to verify that V is a contraction map on $\mathcal{H}(\mathcal{X})$ with the contractive factor $c = \max\{|c_i| : i = 1, 2, \ldots, n-1\}$. Then by the Banach Fixed Point Theorem, V has a unique fixed point (say G) and for any starting set A in $\mathcal{H}(\mathcal{X})$ with $V(A) = V^{\circ 1}(A),\ V^{\circ m}(A) = V \circ V^{\circ m-1}(A)$ for $m \ge 2$,

$$\lim_{m\to\infty} V^{\circ m}(A) = G.$$

This $G \in \mathcal{H}(\mathcal{X})$ is called the attractor or the deterministic fractal of the IFS $\mathcal{I}$, and it is considered as the graph of a FIF in the following case.

2.2 Construction of FIF

Let $x_1 < \cdots < x_n$ be a partition of the real compact interval $I = [x_1, x_n]$. Let a set of data $\triangle = \{(x_i, f_i) \in I \times D : \ i = 1, 2, \ldots, n\}$ be given, where D is a compact set in $\mathbb{R}$. Let $I_i = [x_i, x_{i+1}]$ and $L_i : I \to I_i, \ i = 1, 2, \ldots, n-1$, be contraction homeomorphisms that satisfy

$$L_i(x_1) = x_i, \ L_i(x_n) = x_{i+1}, \tag{1}$$

$$|L_i(e_1) - L_i(e_2)| \leq l_i \ |e_1 - e_2| \ \forall e_1, e_2 \ \in I,$$

for some $0 < l_i < 1$. Let $C = I \times D$ and $F_i : C \to D, \ i = 1, 2, \ldots, n-1$, be continuous such that

$$F_i(x_1, f_1) = f_i, \ F_i(x_n, f_n) = f_{i+1}. \tag{2}$$

$$|F_i(x, y) - F_i(x, z)| \leq |\alpha_i||y - z|, \ x \in I, \ y, z \in D, \ |\alpha_i| < \kappa, \ 0 < \kappa < 1.$$

Now for the construction of an IFS, define the functions $\vartheta_i : C \to I_i \times D \,(\, i = 1, 2, \ldots, n-1)$ as $\vartheta_i(x, f) = (L_i(x), F_i(x, f))$. The construction of a FIF is based on the following result [2].

Proposition 1 *The IFS $\{C; \ \vartheta_i, i = 1, 2, \ldots, n-1\}$ defined above admits a unique attractor G. G is the graph of a continuous function $h^* : I \to D$ such that $h^*(x_i) = f_i$ for $i = 1, 2, \ldots, n$.*

The above function h^* is called a FIF corresponding to the IFS $\{C; \vartheta_i, i = 1, 2, \ldots, n-1\}$, and the construction of h^* is based on the following:

Let $\mathcal{G} = \{g : I \to \mathbb{R} \mid g$ be continuous, $g(x_1) = f_1$ and $g(x_n) = f_n\}$. Then $\mathcal{G}$ is a complete metric space with respect to the metric υ induced by the uniform norm on $\mathcal{C}(I, \mathbb{R})$. Define the Read–Bajraktarević operator T on $(\mathcal{G}, \upsilon)$ as

$$Tg(x) = F_i\left(L_i^{-1}(x), g\left(L_i^{-1}(x)\right)\right), \quad x \in I_i, \quad i = 1, 2, \ldots, n-1. \tag{3}$$

Using (1)–(2), it is easy to verify that Tg is continuous on the interval I_i ; $i = 1, 2, \ldots, n-1$, and at each of the points $x_2, \ldots, x_{n-1}$. Also it is easy to see that T is a contraction map on the metric space $(\mathcal{G}, \upsilon)$, i.e.,

$$\upsilon(Tf, Tg) \leq |\alpha|_\infty \upsilon(f, g), \tag{4}$$

where $|\alpha|_\infty = \max\{|\alpha_i| : i = 1, 2, \ldots, n-1\} < \kappa < 1$. Therefore, by the Banach Fixed Point Theorem, T possesses a unique fixed point h^* (say) on $\mathcal{G}$ such that $(Th^*)(x) = h^*(x) \ \forall \ x \in I$. According to (3), the FIF h^* satisfies the functional equation:

$$h^*(x) = F_i(L_i^{-1}(x), h^* \circ L_i^{-1}(x)), \ x \in I_i, \ i = 1, 2, \ldots, n-1. \tag{5}$$

In the existing constructions of FIFs, $L_i(x)$ and $F_i(x, f)$ in the IFS are defined as

$$\left.\begin{array}{l} L_i(x) = a_i x + b_i, \\ F_i(x, f) = \alpha_i f + r_i(x), \end{array}\right\} \quad i = 1, 2, \dots, n-1, \tag{6}$$

where $-1 < \alpha_i < 1$ and $r_i : I \to \mathbb{R}$ are suitable continuous functions such that (2) is satisfied. α_i is called the scaling factor of the transformation ϑ_i and $\alpha = (\alpha_1, \alpha_2, \dots, \alpha_{n-1})$ is the scale vector of the IFS. The scale vector gives a degree of freedom to the FIF, and allows us to modify its properties. In our construction of the rational cubic FIF, it is assumed that r_i $(i = 1, 2, \dots, n-1)$ are rational functions, where numerators and denominators are cubic polynomials involving two shape parameters.

3 Rational cubic FIFs with two-families of shape parameters

In this section, we construct the rational cubic FIFs with two-families of shape parameters, which generalize a class of classical rational cubic interpolants described in Sarfraz and Hussain [31]. The existence of a spline FIF is given in Barnsley and Harrington [4], and that result can be extended for the existence of rational spline FIFs as prescribed in the following theorem.

Theorem 1 *Let $\{(x_i, f_i), i = 1, 2, \dots, n\}$ be a given data set, where $x_1 < \cdots < x_n$. Suppose that $L_i(x) = a_i x + b_i$, $F_i(x, f) = \alpha_i f + r_i(x)$, $r_i(x) = \frac{p_i(x)}{q_i(x)}$, $p_i(x), q_i(x)$ are suitably chosen polynomials in x of degree M, N, respectively, and $q_i(x) \neq 0$ for every $x \in [x_1, x_n]$. Suppose for some integer $p \geq 0$, $|\alpha_i| < a_i^p$, $i = 1, 2, \dots, n-1$. Let $F_i^m(x, f) = \frac{\alpha_i f + r_i^{(m)}(x)}{a_i^m}$, $r_i^{(m)}$ represents the m^{th} derivative of $r_i(x)$ with respect to x,*

$$f_1^m = \frac{r_1^{(m)}(x_1)}{a_1^m - \alpha_1}, \; f_n^m = \frac{r_{n-1}^{(m)}(x_n)}{a_{n-1}^m - \alpha_{n-1}}, \quad m = 1, 2, \dots, p.$$

$$\textit{If } \; F_i^m(x_n, f_n^m) = F_{i+1}^m(x_1, f_1^m), \quad i = 1, 2, \dots, n-2, \quad m = 1, 2, \dots, p,$$

then $\{\mathbb{R}^2; w_i(x, f) = (L_i(x), F_i(x, f)),\ i = 1, 2, \dots, n-1\}$ determines a rational FIF $\Phi \in \mathcal{C}^p[x_1, x_n]$, and $\Phi^{(m)}$ is the rational FIF determined by $\{\mathbb{R}^2; w_i(x, f) = (L_i(x), F_i^m(x, f)),\ i = 1, 2, \dots, n-1\}$.

Since $q_i(x) \neq 0$ for all $x \in [x_1, x_n]$, the proof of the above theorem follows through the suitable modifications of the arguments in Barnsley and Harrington [4].

3.1 Principle of construction of $\mathcal{C}^1$-rational cubic FIF

Based on the condition on the scaling factors given in the Theorem 1, we now construct the $\mathcal{C}^1$-rational cubic FIFs in the following manner.

Theorem 2 *Let $\{(x_i, f_i), i = 1, 2, \dots, n\}$ be a given data set, where $x_1 < x_2 < \dots < x_n$ and d_i $(i = 1, 2, \dots, n)$ be the derivative values at the knots. Consider the IFS $\mathcal{I}^* = \{\mathbb{R}^2; w_i(x, f) = (L_i(x), F_i(x, f)), i = 1, 2, \dots, n-1\}$, where $L_i(x) = a_i x + b_i$ satisfies (1), $F_i(x, f) = \alpha_i f + r_i(x)$, $r_i(x) = \dfrac{p_i(x)}{q_i(x)}$ contains four real parameters, $p_i(x)$ and $q_i(x)$ are cubic polynomials, $q_i(x) \neq 0\ \forall\ x \in [x_1, x_n]$, and $|\alpha_i| < a_i, i = 1, 2, \dots, n-1$. Let $F_i^1(x, f) = \frac{\alpha_i f + r_i^{(1)}(x)}{a_i}$, where $r_i^{(1)}(x)$ represents the derivative of $r_i(x)$ with respect to x. If*

$$\begin{aligned} &F_i(x_1, f_1) = f_i, F_i(x_n, f_n) = f_{i+1}, \\ &F_i^1(x_1, f_1) = d_i, F_i^1(x_n, f_n) = d_{i+1}, \quad i = 1, 2, \dots, n-1, \end{aligned} \tag{7}$$

then the attractor of the IFS $\mathcal{I}^*$ is the graph of a $\mathcal{C}^1$- rational cubic FIF.

Proof Suppose $\mathcal{U}^* = \{\tau \in \mathcal{C}^1[x_1, x_n] \mid \tau(x_1) = f_1 \text{ and } \tau(x_n) = f_n\}$. Then $(\mathcal{U}^*, d^*)$ is a complete metric space, where d^* is the metric induced by the $\mathcal{C}^1$-norm on $\mathcal{C}^1[x_1, x_n]$. Define the Read–Bajraktarević operator T^* on $\mathcal{U}^*$ as

$$T^*\tau(x) = \alpha_i \tau(L_i^{-1}(x)) + r_i(L_i^{-1}(x)), \quad x \in I_i, \quad i = 1, 2, \dots, n-1. \tag{8}$$

Since $a_i = \frac{x_{i+1} - x_i}{x_n - x_1} < 1$, the condition $|\alpha_i| < a_i < 1$ gives that T^* is a contraction operator on $(\mathcal{U}^*, d^*)$. The fixed point Ψ of T^* is a fractal function that satisfies the functional equation

$$\Psi(L_i(x)) = \alpha_i \Psi(x) + r_i(x), \quad x \in I, \quad i = 1, 2, \dots, n-1. \tag{9}$$

The four real parameters in the rational cubic function $r_i(x)$ are evaluated using (7) in the following way: substituting $x = x_1$ and $x = x_n$ in (9), we get two equations involving f_i and f_{i+1}, respectively, as

$$\left.\begin{aligned} f_i &= \alpha_i f_1 + r_i(x_1), \\ f_{i+1} &= \alpha_i f_n + r_i(x_n), \end{aligned}\right\} \quad i = 1, 2, \dots, n-1. \tag{10}$$

Since $\Psi \in \mathcal{C}^1[x_1, x_n]$, Ψ' satisfies the functional equation:

$$\Psi'(L_i(x)) = \frac{\alpha_i \Psi'(x)}{a_i} + \frac{r_i'(x)}{a_i}, \quad x \in I, \quad i = 1, 2, \dots, n-1. \tag{11}$$

Since $\frac{|\alpha_i|}{a_i} < 1$, Ψ' is a fractal function. Substituting $x = x_1$ and $x = x_n$ in (11), we have two equations involving d_i and d_{i+1}, respectively, as

$$\left.\begin{aligned} d_i &= \frac{\alpha_i d_1}{a_i} + \frac{r_i'(x_1)}{a_i}, \\ d_{i+1} &= \frac{\alpha_i d_n}{a_i} + \frac{r_i'(x_n)}{a_i}, \end{aligned}\right\} \quad i = 1, 2, \dots, n-1. \tag{12}$$

The four real parameters of $r_i(x)$ are determined from (10) and (12). By using similar arguments as in [2], it can be shown that the IFS $\mathcal{I}^*$ has a unique attractor, and it is the graph of the rational cubic FIF $\Psi \in \mathcal{C}^1[x_1, x_n]$.

3.2 Evaluation of $\mathcal{C}^1$-rational cubic FIF with two families of shape parameters

Denote $\triangle_i = \frac{f_{i+1}-f_i}{x_{i+1}-x_i}$. For $i = 1, 2, \ldots, n-1$, assume that

$$p_i(x) \equiv P_i(\theta) = U_i(1-\theta)^3 + M_i\theta(1-\theta)^2 + N_i\theta^2(1-\theta) + Z_i\theta^3,$$
$$q_i(x) \equiv Q_i(\theta) = (1-\theta)^3 + v_i\theta(1-\theta)^2 + w_i\theta^2(1-\theta) + \theta^3,$$

where $\theta = \frac{x-x_1}{x_n-x_1}, x \in [x_1, x_n], v_i > 0$ and $w_i > 0; i = 1, 2, \ldots, n-1$, are shape parameters, and U_i, M_i, N_i and $Z_i, i = 1, 2, \ldots, n-1$, are real parameters to be evaluated. By considering Theorem 2 with above $p_i(x)$ and $q_i(x)$, we take the following functional equation:

$$\Psi(L_i(x)) = \begin{cases} \alpha_i\Psi(x) + \frac{p_i(x)}{q_i(x)}, & \text{if } \triangle_i \neq 0, \\ f_i, & \text{if } \triangle_i = 0. \end{cases} \tag{13}$$

To make the rational cubic fractal function Ψ a $\mathcal{C}^1$-interpolant, one needs to impose the following interpolatory properties:

$$\Psi(x_i) = f_i, \Psi(x_{i+1}) = f_{i+1}, \Psi'(x_i) = d_i, \Psi'(x_{i+1}) = d_{i+1}.$$

Substituting $x = x_1$ in (13), we have

$$\begin{aligned} \Psi(L_i(x_1)) &= \alpha_i\Psi(x_1) + \frac{P_i(0)}{Q_i(0)} \\ \Rightarrow U_i &= f_i - \alpha_i f_1. \end{aligned}$$

Substituting $x = x_n$ in (13), we have

$$\begin{aligned} \Psi(L_i(x_n)) &= \alpha_i\Psi(x_n) + \frac{P_i(1)}{Q_i(1)} \\ \Rightarrow Z_i &= f_{i+1} - \alpha_i f_n. \end{aligned}$$

If $\triangle_i \neq 0$, the condition $\Psi'(x_i) = d_i$ in (13) leads to

$$a_i d_i = \alpha_i\Psi'(x_1) + \frac{Q_i(0)P_i'(0) - Q_i'(0)P_i(0)}{(Q_i(0))^2}.$$

The algebraic manipulation of the above expression gives that

$$M_i = v_i f_i + h_i d_i - \alpha_i[(x_n - x_1)d_1 + f_1 v_i].$$

If $\triangle_i \neq 0$, the condition $\Psi'(x_{i+1}) = d_{i+1}$ in (13) leads to

$$a_i d_{i+1} = \alpha_i \Psi'(x_n) + \frac{Q_i(1)P_i'(1) - Q_i'(1)P_i(1)}{(Q_i(1))^2}.$$

Simplifying this expression for N_i, we have

$$N_i = w_i f_{i+1} - h_i d_{i+1} + \alpha_i[(x_n - x_1)d_n - f_n w_i].$$

Substituting the values of U_i, Z_i, M_i, and N_i in (13), the rational cubic FIF is given by in the following. For $i = 1, 2, \ldots, n-1$,

$$\Psi(L_i(x)) = \begin{cases} \alpha_i \Psi(x) + \frac{P_i(\theta)}{Q_i(\theta)}, & \text{if } \triangle_i \neq 0, \\ f_i, & \text{if } \triangle_i = 0, \end{cases} \tag{14}$$

where

$$\begin{aligned} P_i(\theta) = {} & (f_i - \alpha_i f_1)(1-\theta)^3 + (v_i f_i + h_i d_i - \alpha_i[(x_n - x_1)d_1 + f_1 v_i]) \cdot \\ & \theta(1-\theta)^2 + (w_i f_{i+1} - h_i d_{i+1} + \alpha_i[(x_n - x_1)d_n - f_n w_i]) \cdot \\ & \theta^2(1-\theta) + (f_{i+1} - \alpha_i f_n)\theta^3, \end{aligned}$$

$$Q_i(\theta) = (1-\theta)^3 + v_i\theta(1-\theta)^2 + w_i\theta^2(1-\theta) + \theta^3, \theta = \frac{x - x_1}{x_n - x_1}, x \in [x_1, x_n].$$

In most applications, the derivatives $d_i (i = 1, 2 \ldots, n)$ are not given, and hence must be calculated from the given data by some numerical methods. In this paper, they are computed from the given data in such a way that the $\mathcal{C}^1$- smoothness of the fractal interpolant (14) is retained. These methods are the approximations based on the various mathematical theories in literature, see for instance [9]. We use the following derivative approximations for the shape preserving rational cubic FIFs:
Arithmetic mean method: The three-point difference approximation at internal grids are given as

$$d_i = \begin{cases} 0 & \text{if } \triangle_{i-1} = 0 \text{ or } \triangle_i = 0, \\ \frac{h_i \triangle_{i-1} + h_{i-1}\triangle_i}{h_i + h_{i-1}} & \text{otherwise}, \ \ i = 2, 3, \ldots, n-1, \end{cases}$$

and at the end points, the derivatives are approximated as

$$d_1 = \begin{cases} 0 & \text{if } \triangle_1 = 0 \text{ or } sgn(D_1^*) \neq sgn(\triangle_1), \\ D_1^* = \triangle_1 + \frac{(\triangle_1 - \triangle_2)h_1}{h_1 + h_2} & \text{otherwise}, \end{cases}$$

$$d_n = \begin{cases} 0 & \text{if } \triangle_{n-1} = 0 \text{ or } sgn(D_n^*) \neq sgn(\triangle_{n-1}), \\ D_n^* = \triangle_{n-1} + \frac{(\triangle_{n-1} - \triangle_{n-2})h_{n-1}}{h_{n-1} + h_{n-2}} & \text{otherwise}. \end{cases}$$

Geometric mean method: The non-linear approximations at internal grids are given as

$$d_i = \begin{cases} 0 & \text{if } \triangle_{i-1} = 0 \text{ or } \triangle_i = 0, \\ \triangle_{i-1}^{\frac{h_i}{h_i+h_{i-1}}} \triangle_i^{\frac{h_{i-1}}{h_i+h_{i-1}}} & \text{otherwise}, \ i = 2, 3, \ldots, n-1, \end{cases}$$

and at the end points, the derivatives are approximated as

$$d_1 = \begin{cases} 0 & \text{if } \triangle_1 = 0 \text{ or } \triangle_{3,1} = 0, \\ \triangle_1 \left(\frac{\triangle_1}{\triangle_{3,1}}\right)^{\frac{h_1}{h_2}} & \text{otherwise}, \end{cases}$$

$$d_n = \begin{cases} 0 & \text{if } \triangle_{n-1} = 0 \text{ or } \triangle_{n,n-2} = 0, \\ \triangle_{n-1} \left(\frac{\triangle_{n-1}}{\triangle_{n,n-2}}\right)^{\frac{h_{n-1}}{h_{n-2}}} & \text{otherwise}, \end{cases}$$

where $\triangle_{3,1} = \frac{f_3 - f_1}{x_3 - x_1}$, $\triangle_{n,n-2} = \frac{f_n - f_{n-2}}{x_n - x_{n-2}}$.

The arithmetic mean method is applicable for any real data whereas the geometric mean method is only applicable for monotonically increasing data. For a given bounded data set, the above derivative approximations are bounded, and hence we can use them in the construction of the rational cubic FIF (14).

3.3 Shape control analysis

This section illustrates the effects of the scaling factor α_i, the shape parameters v_i and w_i on the shape of a rational cubic FIF (cf. 14) both mathematically and graphically.

The parameters α_i, v_i and w_i in the rational cubic FIF Ψ can be used to modify the shape of the fractal curve according to the desire of a user for any scientific data. The interval shape control is observed by re-writing the rational cubic FIF Ψ (14) in the following simplified form:

$$\begin{aligned} \Psi(L_i(x)) = \; & \alpha_i \Psi(x) + (f_i - \alpha_i f_1)(1-\theta) + (f_{i+1} - \alpha_i f_n)\theta \\ & + \frac{[(1-\theta)(d_i^* - \triangle_i^*) + \theta(\triangle_i^* - d_{i+1}^*) + \theta(1-\theta)\triangle_i^*(w_i - v_i)]h_i\theta(1-\theta)}{Q_i(\theta)}, \end{aligned} \tag{15}$$

$$\text{where } \; d_i^* = d_i - \frac{\alpha_i d_1}{a_i}, d_{i+1}^* = d_{i+1} - \frac{\alpha_i d_n}{a_i}, \triangle_i^* = \triangle_i - \alpha_i \frac{f_n - f_1}{h_i}.$$

When both v_i and $w_i \to \infty$ in (15), Ψ converges to the following affine FIF:

$$\Psi(L_i(x)) = \alpha_i \Psi(x) + (f_i - \alpha_i f_1)(1-\theta) + (f_{i+1} - \alpha_i f_n)\theta. \tag{16}$$

Again if $\alpha_i \to 0^+$ with $v_i \to \infty$, and $w_i \to \infty$, then the rational cubic FIF modifies to the classical affine interpolant.

Examples: We construct the rational cubic FIFs (see Fig. 1a–c) for the data $\{(0, 0.01), (6, 15), (10, 15), (29.5, 25), (30, 30)\}$ by using the following rational IFS with $n = 5$.

$$\{\mathbb{R}^2; \vartheta_i(x, f) = (L_i(x), F_i(x, f)), i = 1, 2, \ldots, n-1\}, \tag{17}$$

$L_i(x) = a_i x + b_i$, a_i, b_i are evaluated by using (1), and

$$F_i(x, f) = \begin{cases} \alpha_i f + \frac{P_i(\theta)}{Q_i(\theta)}, & \text{if } \triangle_i \neq 0, \\ f_i, & \text{if } \triangle_i = 0, \end{cases}$$

with the expressions of $P_i(\theta)$ and $Q_i(\theta)$ as in (14).

In the construction of the rational cubic FIFs, the choices of the scaling vectors are $\alpha = (0.1,\ 0.1,\ 0.1,\ 0.01)$ in Fig. 1a, b and $\alpha = (0.001,\ 0.001,\ 0.001, 0.001)$ in Fig. 1c. At the knot points, the first order derivatives are approximated by the arithmetic mean method. By analyzing Fig. 1a, b, we conclude that when shape parameters increases, the fractal curve is tightened. In Fig. 1c, α_i is close to zero, and the fractal curve tends to be a piecewise linear interpolant for large values of tension parameters v_i and w_i. Thus, it is verified graphically that as $v_i \to \infty$, $w_i \to \infty$ and $\alpha_i \to 0^+$, both (15) and (16) are same in nature. Hence, the developed rational cubic (14) can be used as a shape preserving fractal interpolant. The effects of shape parameters v_i and w_i are observed by comparing Fig. 1a with Fig. 1b.

Remark 1 By taking $v_i = w_i = 3, \alpha_i = 0$ for $i = 1, 2, \ldots, n-1$ in (14), we get

$$\begin{aligned} \Psi(x) &= (2\rho^3 - 3\rho^2 + 1) f_i + (\rho^3 - 2\rho^2 + \rho) d_i h_i + (-2\rho^3 + 3\rho^2) f_{i+1} \\ &\quad + (\rho^3 - \rho^2) d_{i+1}, \end{aligned}$$

$\rho = \frac{x - x_i}{x_{i+1} - x_i}$, $x \in [x_i, x_{i+1}]$. Now it is easy to see that Ψ is the $\mathcal{C}^1$-Hermite interpolant over $[x_1, x_n]$.

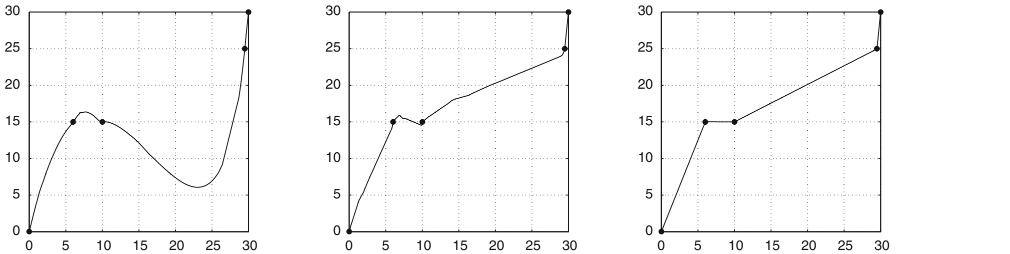

(a) $v_i = w_i = 6$, $\forall i = 1, 2, 3, 4.$ **(b)** $v_i = w_i = 600$, $\forall i = 1, 2, 3, 4.$ **(c)** $v_i = w_i = 6000$, $\forall i = 1, 2, 3, 4.$

Fig. 1 Illustrations of shape control analysis

Remark 2 If $\alpha_i = 0, i = 1, 2, \ldots, n-1$, the rational cubic FIF becomes the classical rational cubic interpolation function $S(x)$ as

$$S(x) = \begin{cases} \frac{f_i(1-\rho)^3+\{v_i f_i+h_i d_i\}\rho(1-\rho)^2+\{w_i f_{i+1}-h_i d_{i+1}\}\rho^2(1-\rho)+f_{i+1}\rho^3}{(1-\rho)^3+v_i\rho(1-\rho)^2+w_i\rho^2(1-\rho)+\rho^3}, & \text{if } \triangle_i \neq 0, \\ f_i, & \text{if } \triangle_i = 0, \end{cases}$$

described in [31], where $x \in [x_i, x_{i+1}]$.

3.4 Approximation properties of rational cubic FIF

In this section, an upper bound of the error between the rational cubic FIF Ψ and an original function $f \in \mathcal{C}^2[x_1, x_n]$ is estimated.

Theorem 3 *Let Ψ and S, respectively, be the rational cubic FIF and classical rational cubic interpolant with respect to the data $\{(x_i, f_i), i = 1, 2, \ldots, n\}$ generated from an original function $f \in \mathcal{C}^2[x_1, x_n]$. Let $d_i, i = 1, 2, \ldots, n$ be the bounded derivatives at the knots. Suppose $V_{n-1} = \bigotimes_{i=1}^{n-1}(-a_i, a_i)$, $|\alpha|_\infty = \max\{|\alpha_i| : i = 1, 2, \ldots, n-1\}$, $h = \max\{h_i : i = 1, 2, \ldots, n-1\}$, and the shape parameters $v_i \geq \Lambda$ and $w_i \geq \Lambda, i = 1, 2, \ldots, n-1$, for some $0 < \Lambda < 1$. Then*

$$\|f - \Psi\|_\infty \leq \frac{|\alpha|_\infty\ (E(h) + E^*(h))}{1 - |\alpha|_\infty} + h^2\ \|f^{(2)}\|_\infty \max_{1 \leq i \leq n-1} c_i,$$

where $E(h) = ||f||_\infty + \frac{2h}{\Lambda}\max\{D_i : i = 1, 2, \ldots, n-1\}$, $E^*(h) = ||f||_\infty + \frac{2h}{\Lambda}\max\{|d_1|, |d_n|\}$, $D_i = \max\{|d_i|, |d_{i+1}|\}$,

$$c_i = \begin{cases} \max\{\ \omega_1(v_i, w_i, \rho)\ :\ \rho \in [0, 1]\ \}, & \text{if } \Lambda \leq w_i < 1, \\ \max\{\ \omega_2(v_i, w_i, \rho)\ :\ \rho \in [0, 1]\ \}, & \text{if } w_i \geq 1, \end{cases}$$

$$\omega_1(v_i, w_i, \rho) = \frac{\rho^2(1-\rho)^2(3 + v_i\rho - v_i(1+\rho))}{2((1-\rho)^3 + v_i\rho(1-\rho)^2 + w_i\rho^2(1-\rho) + \rho^3)},$$

$$\omega_2(v_i, w_i, \rho) = \frac{\rho^2(1-\rho)^2}{2((1-\rho)^3+v_i\rho(1-\rho)^2+v_i\rho^2(1-\rho)+\rho^3)(w_i+(1-w_i)\rho)((v_i-1)\rho+1)}.$$

Proof From (8), the Read–Bajraktarević operator $T_\alpha^* : V_{n-1} \times \mathcal{U}^* \to \mathcal{U}^*$ such that

$$T_\alpha^*\tau(x) = \alpha_i\tau(L_i^{-1}(x)) + \frac{p_i(L_i^{-1}(x), \alpha_i)}{q_i(L_i^{-1}(x))},\ x \in I_i, i = 1, 2, \ldots, n-1, \quad (18)$$

where $p_i(x) \equiv P_i(\theta)$ and $q_i(x) \equiv Q_i(\theta)$ are as in (14). Since Ψ and S, respectively, are the rational cubic FIF and classical cubic spline with respect to the mesh $x_1 < x_2 < \cdots < x_{n-1} < x_n$ interpolating a set of ordinates $\{f_1, f_2, \ldots, f_n\}$ at knots, it is easy to see that Ψ and S are fixed points of the Read–Bajraktarević operator T_α^* for

$\alpha \neq \mathbf{0}$ and $\alpha = \mathbf{0}$, respectively. For $\alpha \neq \mathbf{0}$, T_α^* is a contraction map with contraction factor $|\alpha|_\infty$. Hence

$$\|T_\alpha^*\Psi - T_\alpha^* S\|_\infty \leq |\alpha|_\infty \, \|\Psi - S\|_\infty. \tag{19}$$

Also

$$\begin{aligned}|T_\alpha^* S(x) - T_{\mathbf{0}}^* S(x)| &= |\alpha_i \; S \circ L_i^{-1}(x) + \frac{p_i(L_i^{-1}(x), \alpha_i)}{q_i(L_i^{-1}(x))} - \frac{p_i(L_i^{-1}(x), 0)}{q_i(L_i^{-1}(x))}| \\ &\leq |\alpha_i| \, \|S\|_\infty + \frac{|p_i(L_i^{-1}(x), \alpha_i) - p_i(L_i^{-1}(x), 0)|}{q_i(L_i^{-1}(x))}. \end{aligned} \tag{20}$$

Using the mean value theorem for functions of several variables, there exists $\eta = (\eta_1, \eta_2, \ldots, \eta_{n-1}) \in V_{n-1}$, such that

$$p_i(L_i^{-1}(x), \alpha_i) - p_i(L_i^{-1}(x), 0) = \frac{\partial p_i(L_i^{-1}(x), \eta_i)}{\partial \alpha_i} \alpha_i, \, |\eta_i| < |\alpha_i|. \tag{21}$$

From (20)–(21), we have

$$|T_\alpha^* S(x) - T_{\mathbf{0}}^* S(x)| \leq |\alpha_i| \left(\|S\|_\infty + \left| \frac{\partial \left(\frac{p_i(L_i^{-1}(x), \eta_i)}{q_i(L_i^{-1}(x))} \right)}{\partial \alpha_i} \right| \right). \tag{22}$$

Now we wish to calculate the bounds of each term in the right hand side of (22). From Remark 2, the classical rational cubic interpolant S is re-written as

$$S(x) = w_0^*(v_i, w_i, \rho) f_i + w_1^*(v_i, w_i, \rho) f_{i+1} + w_2^*(v_i, w_i, \rho) d_i - w_3^*(v_i, w_i, \rho) d_{i+1},$$

where

$$\left.\begin{aligned} w_0^*(v_i, w_i, \rho) = \tfrac{(1-\rho)^3 + \rho(1-\rho)^2 v_i}{Q_i(\rho)}, \; w_1^*(v_i, w_i, \rho) = \tfrac{\rho^2(1-\rho)w_i + \rho^3}{Q_i(\rho)}, \\ w_2^*(v_i, w_i, \rho) = \tfrac{\rho(1-\rho)^2 h_i d_i}{Q_i(\rho)}, \; w_3^*(v_i, w_i, \rho) = \tfrac{\rho^2(1-\rho) h_i d_{i+1}}{Q_i(\rho)}. \end{aligned}\right\} \tag{23}$$

Now it is easy to see that

$$w_0^*(v_i, w_i, \rho) + w_1^*(v_i, w_i, \rho) = 1. \tag{24}$$

Also

$$\begin{aligned} w_2^*(v_i, w_i, \rho) + w_3^*(v_i, w_i, \rho) &= \frac{\rho(1-\rho)^2 h_i + \rho^2(1-\rho) h_i}{Q_i(\rho)} \\ &\leq \frac{\rho(1-\rho)^2 h_i + \rho^2(1-\rho) h_i}{v_i \rho (1-\rho)^2 + w_i \rho^2 (1-\rho)} \end{aligned}$$

$$\leq \frac{h_i}{v_i} + \frac{h_i}{w_i}$$
$$\leq \frac{2h_i}{\Lambda}. \tag{25}$$

From (23)–(25), we have

$$|S(x)| \leq \max\{|f_i|, |f_{i+1}|\} + \frac{2h_i}{\Lambda} \max\{|d_i|, |d_{i+1}|\}$$
$$\leq ||f||_\infty + \frac{2h_i}{\Lambda} \max\{|d_i|, |d_{i+1}|\}.$$

Since the above inequality is true for all $i = 1, 2, \ldots, n-1$, we get the following estimation:

$$\|S\|_\infty \leq E(h). \tag{26}$$

Since $q_i(x)$ is independent of α_i, we have

$$\frac{\partial\left(\frac{p_i(L_i^{-1}(x),\alpha_i)}{q_i(L_i^{-1}(x))}\right)}{\partial\alpha_i} = -w_0^*(v_i, w_i, \rho) f_1 - w_1^*(v_i, w_i, \rho) f_n - w_2^*(v_i, w_i, \rho) d_1$$
$$+ w_3^*(v_i, w_i, \rho) d_n.$$

Now by using a similar argument used in the estimation of $\|S\|_\infty$, we can show that

$$\left|\frac{\partial\left(\frac{p_i(L_i^{-1}(x),\alpha_i)}{q_i(L_i^{-1}(x))}\right)}{\partial\alpha_i}\right| \leq \max\{|f_1|, |f_n|\} + \frac{2h_i}{\Lambda} \max\{|d_1|, |d_n|\}$$
$$\leq ||f||_\infty + \frac{2h_i}{\Lambda} \max\{|d_1|, |d_n|\}.$$

Since the above equation is true for all $i = 1, 2, \ldots, n-1$, we get the following estimation:

$$\left|\frac{\partial\left(\frac{p_i(L_i^{-1}(x),\alpha_i)}{q_i(L_i^{-1}(x))}\right)}{\partial\alpha_i}\right| \leq E^*(h). \tag{27}$$

Substituting (26)–(27) in (22), we obtain

$$|T_\alpha^* S(x) - T_{\mathbf{0}}^* S(x)| \leq |\alpha|_\infty \, (E(h) + E^*(h)).$$

This implies

$$\|T_\alpha^* S - T_{\mathbf{0}}^* S\|_\infty \le |\alpha|_\infty \, (E(h) + E^*(h)). \tag{28}$$

Using (19) and (28) together with inequality

$$\|\Psi - S\|_\infty = \|T_\alpha^* \Psi - T_{\mathbf{0}}^* S\|_\infty \le \|T_\alpha^* \Psi - T_\alpha^* S\|_\infty + \|T_\alpha^* S - T_{\mathbf{0}}^* S\|_\infty \tag{29}$$

gives that

$$\|\Psi - S\|_\infty \le \frac{|\alpha|_\infty \, (E(h) + E^*(h))}{1 - |\alpha|_\infty}. \tag{30}$$

Also from [12], it is known that

$$\|f - S\|_\infty \le \|f^{(2)}\|_\infty \max_{1 \le i \le n-1} \{h_i^2 c_i\} = h^2 \, \|f^{(2)}\|_\infty \max_{1 \le i \le n-1} c_i. \tag{31}$$

Using (30)–(31) together with inequality

$$\|\Psi - f\|_\infty \le \|\Psi - S\|_\infty + \|S - f\|_\infty, \tag{32}$$

we have obtained the desired bound for $\|\Psi - f\|_\infty$.

Convergence results: Assume that $E(h)$ and $E^*(h)$ remain bounded for every small value of h. Then since $|\alpha|_\infty < \frac{h}{x_n - x_1}$, Theorem 3 gives that the rational cubic FIF converges uniformly to the original function f as $h \to 0$. Also it is possible to get $O(h^2)$ convergence with a choice of the scaling factors $|\alpha_i| < a_i^2$, $i = 1, 2, \ldots, n-1$ using the same assumptions on $E(h)$ and $E^*(h)$.

4 Shape preserving fractal interpolation

For an arbitrary selection of the scaling factors and shape parameters, the rational cubic FIF Ψ described in Sect. 3.2 may not be either monotonic (for instance see Fig. 1a, b), positive, or convex (concave), if the data set is either monotonic, positive, or convex (concave), respectively. This is very similar to the ordinary spline schemes that do not provide the desired shape features of a data. Thus some mathematical treatment is required to achieve a monotonicity, positivity, and convexity (concavity) preserving rational cubic spline FIF for a given data which is monotonic, positive, and convex (concave), respectively. One way to achieve the shape preserving interpolant by the above rational cubic IFS scheme, is to play with the scaling factors and shape parameters on trial and error basis in those regions of the fractal curve, where the shape violations are found. But this is not a comfortable and accurate way to manipulate the desired shape preserving fractal curve. Another way that is more effective, useful, and is the objective of this section, is the automated generation of a shape preserving rational cubic FIF. This requires an automated computation of the suitable scaling factors and shape parameters from the prescribed data. To proceed with this strategy, the sufficient conditions in terms of the scaling factors and shape parameters are derived in Sects. 4.1, 4.2, and 4.3, respectively, for the monotonicity, positivity, and convexity (concavity) preserving rational cubic FIFs.

4.1 Sufficient conditions for monotonicity

Theorem 4 *Let $\{(x_i, f_i, d_i), i = 1, 2, \ldots, n\}$ be a given monotonic data. Let the derivative values satisfy the necessary conditions for monotonicity, namely*

$$\begin{cases} d_i = d_{i+1} = 0 & \text{for } \triangle_i = 0, \\ sgn(d_i) = sgn(d_{i+1}) = sgn(\triangle_i) & \text{for } \triangle_i \neq 0. \end{cases} \tag{33}$$

If (i) *the scaling factors α_i, $i = 1, 2, \ldots, n-1$, are chosen as*

$$\alpha_i \in \begin{cases} [0, \mu_i], & \text{if } \mu_i < a_i, \\ [0, a_i), & \text{if } \mu_i \geq a_i, \quad \text{where } \ \mu_i = min\{\frac{a_i d_i}{d_1}, \frac{a_i d_{i+1}}{d_n}, \frac{f_{i+1}-f_i}{f_n - f_1}\}, \end{cases} \tag{34}$$

(ii) *the shape parameters v_i and w_i, $i = 1, 2, \ldots, n-1$, are selected as either*

$$v_i = \frac{l_i d_i^*}{\triangle_i^*}, \ w_i = \frac{k_i d_{i+1}^*}{\triangle_i^*}, \text{ where } l_i, k_i \in \mathbb{R}^+ \text{ such that } \frac{1}{l_i} + \frac{1}{k_i} \leq 1, \ \text{ and } \triangle_i^* \neq 0, \tag{35}$$

or

$$v_i = \eta_i \left(\frac{d_i^* + d_{i+1}^*}{\triangle_i^*} \right), \ w_i = \nu_i \left(\frac{d_i^* + d_{i+1}^*}{\triangle_i^*} \right) \text{provided } d_i^* \neq 0, \ d_{i+1}^* \neq 0, \ \text{ and } \triangle_i^* \neq 0, \tag{36}$$

where $\eta_i \geq 1$ and $\nu_i \geq 1$, $d_i^* = d_i - \frac{\alpha_i d_1}{a_i}$, $d_{i+1}^* = d_{i+1} - \frac{\alpha_i d_n}{a_i}$, $\triangle_i^* = \triangle_i - \alpha_i \frac{f_n - f_1}{h_i}$, then for fixed α_i, v_i, and w_i, $i = 1, 2, \ldots, n-1$, there exists a unique monotonicity preserving $\mathcal{C}^1$-rational cubic FIF Ψ (14) such that its graph is the attractor of the rational cubic IFS (17).

Proof From the calculus of single variable functions, Ψ is monotonic if and only if $\Psi'(x) \geq 0$ (for monotonically increasing data) or $\Psi'(x) \leq 0$ (for monotonically decreasing data) for all $x \in (x_1, x_n)$. Differentiating (14) with respect to x, after some rigorous calculations, we get the following expression:

$$\Psi'(L_i(x)) = \frac{\alpha_i \Psi'(x)}{a_i} + \frac{\Omega_i(\theta)}{(Q_i(\theta))^2}, \tag{37}$$

where

$$\Omega_i(\theta) = \sum_{j=1}^{6} A_{j,i} \theta^{j-1} (1-\theta)^{6-j},$$

$$
\begin{aligned}
A_{1,i} &= d_i^*,\\
A_{2,i} &= 2w_i\left(\triangle_i^* - \frac{d_{i+1}^*}{w_i}\right) + d_i^*,\\
A_{3,i} &= 3\triangle_i^* + 2w_i\left(\triangle_i^* - \frac{d_{i+1}^*}{w_i}\right) + w_i v_i\left(\triangle_i^* - \frac{d_i^*}{v_i} - \frac{d_{i+1}^*}{w_i}\right),\\
A_{4,i} &= 3\triangle_i^* + 2v_i\left(\triangle_i^* - \frac{d_i^*}{v_i}\right) + w_i v_i\left(\triangle_i^* - \frac{d_i^*}{v_i} - \frac{d_{i+1}^*}{w_i}\right),\\
A_{5,i} &= 2v_i\left(\triangle_i^* - \frac{d_i^*}{v_i}\right) + d_{i+1}^*,\\
A_{6,i} &= d_{i+1}^*.
\end{aligned}
$$

Due to the recursive nature of Ψ' and coefficients in $\Omega_i(\theta)$, the above necessary conditions (33) are not sufficient to ensure monotonicity of a rational cubic FIF Ψ for arbitrary values of parameters α_i, v_i, and w_i, $i = 1, 2, \ldots, n-1$. Therefore we derive the sufficient conditions through the scaling factors α_i and shape parameters v_i, w_i, $i = 1, 2, \ldots, n-1$, so that these conditions together with the above necessary conditions give monotonicity capturing rational cubic FIFs.

Case-I: monotonically increasing data

Let $\{(x_i, f_i), i = 1, 2, \ldots, n\}$ be a given monotonically increasing data set. Since $(Q_i(\theta))^2 > 0$ for every $\theta \in [0, 1]$, the non-negativity of $\dfrac{\Omega_i(\theta)}{(Q_i(\theta))^2}$ (cf. 37) depends on the non-negativity of $\Omega_i(\theta)$ for $\theta \in [0, 1]$. Thus the problem reduces to the determination of α_i, v_i, and w_i for which the polynomial $\Omega_i(\theta)$ is non-negative for all $i = 1, 2, \ldots, n-1$.

From (37), it is easy to verify that $\Omega_i(\theta) \geq 0$ for $\theta \in [0, 1]$ if

$$A_{j,i} \geq 0, \quad j = 1, 2, \ldots, 6.$$

$$\text{Now } A_{1,i} = d_i^* \geq 0 \Leftrightarrow d_i - \frac{\alpha_i d_1}{a_i} \geq 0 \;\Leftrightarrow \alpha_i \leq \frac{a_i d_i}{d_1}.$$

$$\text{Similarly, } A_{6,i} = d_{i+1}^* \geq 0 \Leftrightarrow \alpha_i \leq \frac{a_i d_{i+1}}{d_n},\;\; \triangle_i^* \geq 0 \Leftrightarrow \alpha_i \leq \frac{f_{i+1} - f_i}{f_n - f_1}.$$

Also from the calculus of FIFs [4], we have $\Psi \in \mathcal{C}^1[x_1, x_n]$ whenever $-a_i < \alpha_i < a_i$.

Therefore, $\Psi \in \mathcal{C}^1[x_1, x_n]$, $A_{1,i} = d_i^* \geq 0$, $A_{6,i} = d_{i+1}^* \geq 0$, and $\triangle_i^* \geq 0$ if

$$\alpha_i \in \begin{cases} (-a_i, \mu_i], & \text{if } \mu_i < a_i,\\ (-a_i, a_i), & \text{if } \mu_i \geq a_i. \end{cases} \tag{38}$$

Next we make each term of $A_{j,i}$, $j = 2, 3, 4, 5$ to be non-negative. It is easy to verify that including (38), with restrictions $v_i \geq 0$, $w_i \geq 0$, the sufficient conditions for $A_{j,i} \geq 0$, $j = 2, 3, 4, 5$ are

$$\triangle_i^* - \frac{d_i^*}{v_i} \geq 0, \triangle_i^* - \frac{d_{i+1}^*}{w_i} \geq 0, \triangle_i^* - \frac{d^*}{v_i} - \frac{d_{i+1}^*}{w_i} \geq 0. \tag{39}$$

Let $v_i = \frac{l_i d_i^*}{\triangle_i^*}$, $w_i = \frac{k_i d_{i+1}^*}{\triangle_i^*}$, $l_i, k_i \in \mathbb{R}^+$. Using these expressions,

$$\left.\begin{aligned} \triangle_i^* - \tfrac{d_i^*}{v_i} &= \triangle_i^*(1 - \tfrac{1}{l_i}), \\ \triangle_i^* - \tfrac{d_{i+1}^*}{w_i} &= \triangle_i^*(1 - \tfrac{1}{k_i}), \\ \triangle_i^* - \tfrac{d_i^*}{v_i} - \tfrac{d_{i+1}^*}{w_i} &= \triangle_i^*(1 - \tfrac{1}{l_i} - \tfrac{1}{k_i}). \end{aligned}\right\} \tag{40}$$

From (40), we observe that inequalities (39) are true if the shape parameters chosen according to (35).

If $d_i^* \neq 0$ and $d_{i+1}^* \neq 0$, (35) leads to the following sufficient conditions:

$$l_i \geq 1 + \frac{d_{i+1}^*}{d_i^*}, k_i \geq 1 + \frac{d_i^*}{d_{i+1}^*}.$$

Substituting above inequalities in (35), we have the following conditions on the shape parameters:

$$v_i \geq \frac{d_i^* + d_{i+1}^*}{\triangle_i^*}, \quad w_i \geq \frac{d_i^* + d_{i+1}^*}{\triangle_i^*}. \tag{41}$$

It is easy to see that inequalities in (41) are true whenever (36) is true.

Therefore the rational cubic FIF $\Psi \in \mathcal{C}^1[x_1, x_n]$, and expression $\dfrac{\Omega_i(\theta)}{(Q_i(\theta))^2} \geq 0$ (cf. 37) if the scaling factors and shape parameters obey (38) and (35) or (36), respectively.

With the above observation if $\alpha_i \geq 0$ (chosen with respect to 38) and $\Psi'(x_j) \geq 0, \forall j = 1, 2, \ldots, n$, then it is easy to verify that $\Psi'(L_i(x_j)) \geq 0$, $j = 1, 2, \ldots, n$, $i = 1, 2, \ldots, n-1$. Since $\{\mathbb{R}; L_i(x), i = 1, 2, \ldots, n-1\}$ is the IFS for $[x_1, x_n]$, we have $\Psi'(x) \geq 0$ for all $x \in [x_1, x_n]$.

Otherwise, if $\alpha_i < 0$ (chosen with respect to 38), due to the implicit structure of Ψ', we may not ensure that $\Psi'(L_i(x)) \geq 0$ for every $x \in [x_1, x_n]$ even if $\frac{\Omega_i(\theta)}{Q_i^2(\theta)} \geq 0$. To avoid this uncertainty, we choose the scaling vector $\alpha = (\alpha_1, \alpha_2, \ldots, \alpha_{n-1})$ as

$$\alpha_i \in \begin{cases} [0, \mu_i], & \text{if } \mu_i < a_i, \\ [0, a_i), & \text{if } \mu_i \geq a_i. \end{cases}$$

From the above discussion, we conclude that the selections of the scaling factors and shape parameters according to (34) and (35) or (36) are sufficient to obtain a monotonically increasing rational cubic FIF Ψ for a given monotonically increasing data.

Case-II : monotonically decreasing data

Let $\{(x_i, f_i), i = 1, 2, \ldots, n\}$ be a given monotonically decreasing data set, hence $\triangle_i \leq 0$. Since $(Q_i(\theta))^2 > 0$, $\dfrac{\Omega_i(\theta)}{(Q_i(\theta))^2} \leq 0 \Leftrightarrow \Omega_i(\theta) \leq 0$ for every $\theta \in [0, 1]$. After some simple calculations, it is found that $\Omega_i(\theta) \le 0$ if the scaling factors and shape parameters obey (38) and either (35) or (36), respectively. If $\alpha_i \ge 0$ (chosen with respect to 38), then it is easy to verify that $\Psi'(L_i(x)) \le 0$ for every $x \in [x_1, x_n]$, $i = 1, 2, \ldots, n-1$. Otherwise, if $\alpha_i < 0$ (chosen with respect to 38), due to the implicit structure of Ψ', we may not ensure that $\Psi'(L_i(x)) \le 0$ for every $x \in [x_1, x_n]$ even if $\frac{\Omega_i(\theta)}{Q_i^2(\theta)} \le 0$. To avoid this uncertainty, choose the scaling vector with respect to (34), and then the shape parameters by (35) or (36).

From the above discussion, we conclude that selections of the scaling factors and shape parameters according to (34) and (35) or (36) are sufficient to obtain the monotonically decreasing rational cubic FIF Ψ for a given monotonically decreasing data. Furthermore, the uniqueness of a monotonic rational cubic FIF Ψ for a fixed $\alpha_i, v_i, w_i, i = 1, 2, \ldots, n-1$, follows from the fixed point theorem. Hence the theorem is proved from the arguments of Case-I and Case-II.

Remark 3 In Theorem 4, we have assumed $f_1 \ne f_n$. If $f_1 = f_n$, there is nothing to discuss, and in this case our rational cubic FIF will be a constant function with constant value f_1 throughout the interval $[x_1, x_n]$, and the scaling vector is zero. If any term in the calculation of μ_i in (34) is indeterminate, then ignore that ratio for the calculation of α_i.

4.2 Sufficient conditions for positivity

Theorem 5 *Let $\{(x_i, f_i, d_i), i = 1, 2, \ldots, n\}$ be a given positive data. If*

(i) *the scaling factors $\alpha_i, i = 1, 2, \ldots, n-1$, are chosen as*

$$\alpha_i \in \left[0, \min\left\{a_i, \frac{f_i}{f_1}, \frac{f_{i+1}}{f_n}\right\}\right), \tag{42}$$

(ii) *the shape parameters v_i and w_i, $i = 1, 2, \ldots, n-1$, are selected as*

$$\begin{cases} u_i > 0, & \text{if } d_i^* \le 0, \\ u_i > \frac{h_i d_i^*}{t_{4,i}^*}, & \text{if } d_i^* > 0, \\ w_i > 0, & \text{if } d_{i+1}^* \le 0, \\ w_i > \frac{h_i d_{i+1}^*}{t_{1,i}^*}, & \text{if } d_{i+1}^* > 0, \end{cases} \tag{43}$$

where

$$t_{1,i}^* = f_{i+1} - \alpha_i f_n, t_{4,i}^* = f_i - \alpha_i f_1, d_i^* = d_i - \frac{\alpha_i d_1}{a_i}, d_{i+1}^* = d_{i+1} - \frac{\alpha_i d_n}{a_i},$$

then for a fixed $\alpha_i, v_i, w_i, i = 1, 2, \ldots, n-1$, there exists a unique positivity preserving $\mathcal{C}^1$-rational cubic FIF Ψ (14) such that its graph is the attractor of the rational cubic IFS (17).

Proof From (14), we have

$$\Psi(L_i(x)) = \alpha_i \Psi(x) + \frac{P_i(\theta)}{Q_i(\theta)}, \theta = \frac{x - x_1}{x_n - x_1}, x \in [x_1, x_n].$$

It is easy to verify that for $i = 1, 2, \ldots, n-1$, if $\alpha_i \geq 0$, the sufficient condition for $\Psi(L_i(x)) > 0$ for all $x \in [x_1, x_n]$ is

$$\frac{P_i(\theta)}{Q_i(\theta)} > 0 \quad \text{for all } \theta \in [0, 1].$$

So initial conditions on the scaling factors are $\alpha_i \geq 0, i = 1, 2, \ldots, n-1$. Since $Q_i(\theta) > 0 \ \forall \ \theta \in [0, 1]$ for $v_i > 0, w_i > 0, i = 1, 2, \ldots, n-1$, the positivity of the rational function $\frac{P_i(\theta)}{Q_i(\theta)}$ depends on the positivity of $P_i(\theta)$. Next our aim is the determination of appropriate values of α_i, v_i, and w_i for which the polynomial $P_i(\theta)$ is positive. From (14), $P_i(\theta)$ is re-written as

$$P_i(\theta) = t_{1,i}\theta^3 + t_{2,i}\theta^2 + t_{3,i}\theta + t_{4,i}, \tag{44}$$

where

$$\begin{aligned}
t_{1,i} &= (1 - w_i)(f_{i+1} - \alpha_i f_n) - (1 - v_i)(f_i - \alpha_i f_1) + (d^*_{i+1} + d^*_i)h_i, \\
t_{2,i} &= w_i(f_{i+1} - \alpha_i f_n) - (3 - 2v_i)(f_i - \alpha_i f_1) - (d^*_{i+1} + d^*_i)h_i, \\
t_{3,i} &= d^*_i h_i - (3 - v_i)(f_i - \alpha_i f_1), \\
t_{4,i} &= (f_i - \alpha_i f_1).
\end{aligned}$$

By substituting $\theta = \frac{s}{s+1}$ in (44), $P_i(\theta) > 0$ for all $\theta \in [0, 1]$ is equivalent to

$$\Omega_i(s) = t^*_{1,i}s^3 + t^*_{2,i}s^2 + t^*_{3,i}s + t^*_{4,i} > 0 \quad \text{for all } s \geq 0,$$

where $t^*_{1,i} = t_{1,i}+t_{2,i}+t_{3,i}+t_{4,i}$, $t^*_{2,i} = t_{2,i}+2t_{3,i}+3t_{4,i}$, $t^*_{3,i} = t_{3,i}+3t_{4,i}$, $t^*_{4,i} = t_{4,i}$. From [33], we have $\Omega_i(s) > 0$ for all $s \geq 0$ if and only if $(t^*_{1,i}, t^*_{2,i}, t^*_{3,i}, t^*_{4,i}) \in R_1 \cup R_2$, where

$$\begin{aligned}
R_1 &= \{(t^*_{1,i}, t^*_{2,i}, t^*_{3,i}, t^*_{4,i}) : t^*_{1,i} > 0, t^*_{2,i} > 0, t^*_{3,i} > 0, t^*_{4,i} > 0\}, \\
R_2 &= \{(t^*_{1,i}, t^*_{2,i}, t^*_{3,i}, t^*_{4,i}) : t^*_{1,i} > 0, t^*_{4,i} > 0, 4t^*_{1,i}t^*_{3,i} + 4t^*_{4,i}t^*_{2,i} + 27t^{*2}_{1,i}t^{*2}_{4,i} \\
&\qquad -18t^*_{1,i}t^*_{2,i}t^*_{3,i}t^*_{4,i} - t^*_{2,i}t^*_{3,i} > 0\}, \\
t^*_{1,i} &= f_{i+1} - \alpha_i f_n, \ \ t^*_{2,i} = w_i(f_{i+1} - \alpha_i f_n) - h_i d^*_{i+1}, \\
t^*_{3,i} &= v_i(f_i - \alpha_i f_1) + h_i d^*_i, \ \ t^*_{4,i} = f_i - \alpha_i f_1.
\end{aligned}$$

Let $(t^*_{1,i}, t^*_{2,i}, t^*_{3,i}, t^*_{4,i}) \in R_1$, then we have

$$t^*_{1,i} > 0, t^*_{2,i} = w_i t^*_{1,i} - h_i d^*_{i+1} > 0, t^*_{4,i} > 0, t^*_{3,i} = v_i t^*_{4,i} + h_i d^*_i > 0.$$

Now, it is easy to see that $t^*_{1,i} > 0$ and $t^*_{4,i} > 0$ if and only if

$$\alpha_i < \min\left\{\frac{f_i}{f_1}, \frac{f_{i+1}}{f_n}\right\}. \tag{45}$$

If $d^*_{i+1} \leq 0$, $t^*_{2,i} > 0$ is true due to (45), and in this case $w_i > 0$ can be chosen arbitrarily. Otherwise $d^*_{i+1} > 0$ and we have $w_i t^*_{1,i} - h_i d^*_{i+1} > 0$ if and only if $w_i > \frac{h_i d^*_{i+1}}{t^*_{1,i}}$.

Similarly, $v_i t^*_{4,i} + h_i d^*_i > 0$ is valid when (i) $d^*_i \geq 0$, choose $v_i > 0$ arbitrarily (ii) $d^*_i < 0$, choose $v_i > \frac{-h_i d^*_i}{t^*_{4,i}}$. Due to the complexity in calculations, we have omitted the region R_2. The above discussions yield (43). Therefore $P_i(\theta) > 0$ if (45) and (43) are true.

Now it is easy to verify that a $\mathcal{C}^1$- rational cubic FIF Ψ is positive if the scaling factors and shape parameters involved in the IFS (17) are chosen according to (42) and (43), respectively.

4.3 Sufficient conditions for convexity

An interpolation data set $\{(x_i, f_i), i = 1, 2, \ldots, n\}$ is said to be convex (concave) if

$$\begin{gathered}\triangle_1 \leq \triangle_2 \leq \cdots \leq \triangle_{i-1} \leq \triangle_i \leq \cdots \leq \triangle_{n-1}\\ (\triangle_1 \geq \triangle_2 \geq \cdots \geq \triangle_{i-1} \geq \triangle_i \geq \cdots \geq \triangle_{n-1}).\end{gathered}$$

Theorem 6 *Let* $\{(x_i, f_i, d_i), i = 1, 2, \ldots, n\}$ *be a given convex (concave) data, where* f_i *and* d_i *are value and slope of twice differentiable function at* x_i*, respectively. Let the derivatives satisfy the necessary conditions for convexity (concavity), namely*

$$\begin{gathered}d_1 \leq \triangle_1 \leq d_2 \leq \triangle_2 \leq \cdots \leq \triangle_{i-1} \leq d_i \leq \triangle_i \leq \cdots \leq \triangle_{n-1} \leq d_n\\ (d_1 \geq \triangle_1 \geq d_2 \geq \triangle_2 \geq \cdots \geq \triangle_{i-1} \geq d_i \geq \triangle_i \geq \cdots \geq \triangle_{n-1} \geq d_n).\end{gathered} \tag{46}$$

Suppose (i) *the scaling factors* α_i, $i = 1, 2, \ldots, n-1$, *are chosen as*

$$\left.\begin{aligned}&\alpha_i \in [0, \mu^*_i], \mu^*_i = min\{a_i^2, \tfrac{e_{1,i}}{\Theta_1}, \tfrac{f_{1,i}}{\Theta_2}, \tfrac{h_{1,i}}{\Theta_3}\}\ if\ \Theta_1 \neq 0, \Theta_2 \neq 0,\ and\ \Theta_3 \neq 0\\ &(if\ any\ \ \Theta_i = 0\ for\ i = 1, 2, 3,\ then\ ignore\ the\ corresponding\ fraction\ in\ \mu^*_i),\end{aligned}\right\} \tag{47}$$

where

$$e_{1,i} = (\triangle_i - d_i)h_i,\ f_{1,i} = (d_{i+1} - \triangle_i)h_i,\ \ h_{1,i} = (d_{i+1} - d_i)a_i,$$

$$\Theta_1 = f_n - f_1 - (x_n - x_1)d_1, \Theta_2 = (x_n - x_1)d_n - (f_n - f_1), \Theta_3 = d_n - d_1,$$

(ii) *the shape parameters* v_i *and* w_i, $i = 1, 2, \ldots, n-1$, *are selected as*

$$\left.\begin{array}{l} v_i = w_i \geq max\{\frac{d^*_{i+1}-d^*_i}{\triangle^*_i-d^*_i}, \frac{d^*_{i+1}-d^*_i}{d^*_{i+1}-\triangle^*_i}\}\ provided\ \triangle_i - d_i \neq 0\ and\ d_{i+1} - \triangle_i \neq 0, \\ (if\ either\ \triangle_i - d_i = 0\ or\ d_{i+1} - \triangle_i = 0, then\ take\ \alpha_i = 0, d_i = d_{i+1} = \triangle_i, \\ and\ no\ need\ to\ choose\ v_i,\ and\ w_i), \end{array}\right\} \tag{48}$$

where $d^*_i = d_i - \frac{\alpha_i d_1}{a_i}$, $d^*_{i+1} = d_{i+1} - \frac{\alpha_i d_n}{a_i}$, $\triangle^*_i = \triangle_i - \alpha_i \frac{f_n - f_1}{h_i}$.

Then for a fixed $\alpha_i, v_i, w_i, i = 1, 2, \ldots, n-1$, *there exists a unique convexity (concavity) preserving* $\mathcal{C}^1$*-rational cubic FIF* Ψ (14) *such that its graph is the attractor of the rational cubic IFS* (17).

Proof Without loss of generality, we consider a convex data set. From the calculus of single variable functions, the rational cubic FIF Ψ is convex if and only if $\Psi''(x) \geq 0\ \forall\, x \in [x_1, x_n]$. Differentiating (37) with respect to x, after some rigorous calculations, we get the following expressions using the notations from Sect. 4.1.

$$\Psi''(L_i(x)) = \frac{\alpha_i \Psi''(x)}{a_i^2} + \frac{\Omega^*_i(\theta)}{h_i(Q_i(\theta))^3},\ \ \Omega^*_i(\theta) = \sum_{j=1}^{8} A^*_{j,i}\theta^{j-1}(1-\theta)^{6-j}, \tag{49}$$

where

$$\left.\begin{array}{l} A^*_{1,i} = A_{2,i} - A_{1,i}(2v_i - 1), \\ A^*_{2,i} = 2A_{3,i} - A_{2,i}(v_i - 2) - A_{1,i}(v_i + 4w_i), \\ A^*_{3,i} = 3A_{4,i} + A_{3,i} - 3w_i A_{2,i} - 3A_{1,i}(w_i + 2), \\ A^*_{4,i} = 4A_{5,i} + 4A_{4,i}(v_i + 1) + A_{3,i}(v_i - 2w_i) - A_{2,i}(2w_i + 5) - 5A_{1,i}, \\ A^*_{5,i} = 5A_{6,i} + A_{5,i}(2v_i + 5) + A_{4,i}(2v_i - w_i) - A_{3,i}(w_i - 4) - 4A_{2,i}, \\ A^*_{6,i} = 3A_{6,i}(v_i + 2) + 3v_i A_{5,i} - 3A_{4,i} - 3A_{3,i}, \\ A^*_{7,i} = A_{6,i}(4v_i + w_i) + A_{5,i}(w_i - 2) - 2A_{4,i}, \\ A^*_{8,i} = A_{6,i}(2w_i - 1) - A_{5,i}. \end{array}\right\} \tag{50}$$

If $\alpha_i \geq 0, i = 1, 2, \ldots, n-1$, then it is easy to see that $\Psi''(x) \geq 0$ for all $x \in [x_1, x_n]$ if

$$\frac{\Omega^*_i(\theta)}{(Q_i(\theta))^3} \geq 0 \quad \text{for all} \ \ \theta \in [0, 1].$$

Thus an initial condition on the scaling factor is $\alpha_i \geq 0, i = 1, 2, \ldots, n-1$. Since $(Q_i(\theta))^3 > 0$ for $v_i > 0$ and $w_i > 0, i = 1, 2, \ldots, n-1$, the non-negativity of $\frac{\Omega^*_i(\theta)}{(Q_i(\theta))^3}$ depends on the non-negativity of $\Omega^*_i(\theta)$ in the interval $[0, 1]$. Thus, the problem reduces to the determination of appropriate restrictions on the parameters α_i, v_i, and w_i, $i = 1, 2, \ldots, n-1$, for which $\Omega^*_i(\theta) \geq 0$. Next from (50), it is easy to see that the sufficient conditions for $\Omega^*_i(\theta) \geq 0\ \forall\, \theta \in [0, 1]$ are $A^*_{j,i} \geq 0$ for all $j = 1, 2, \ldots, 8$. After some simplifications, $A^*_{1,i}$ and $A^*_{8,i}$ in (50) are re-written, respectively, as

$$\left.\begin{array}{l} A^*_{1,i} = 2\{(w_i - v_i)\triangle^*_i + v_i(\triangle^*_i - d^*_i) - (d^*_{i+1} - d^*_i)\}, \\ A^*_{8,i} = 2\{(w_i - v_i)\triangle^*_i + w_i(d^*_{i+1} - \triangle^*_i) - (d^*_{i+1} - d^*_i)\}, \end{array}\right\} \tag{51}$$

where

$$\left.\begin{array}{ll} \triangle_i^* - d_i^* & = \triangle_i - d_i - \alpha_i \frac{f_n - f_1 - (x_n - x_1) d_1}{h_i}, \\ d_{i+1}^* - \triangle_i^* & = (d_{i+1} - \triangle_i) - \alpha_i \frac{(x_n - x_1) d_n - (f_n - f_1)}{h_i}, \\ d_{i+1}^* - d_i^* & = d_{i+1} - d_i - \alpha_i \frac{d_n - d_1}{a_i}. \end{array}\right\} \tag{52}$$

Applying the three chords lemma for the convex functions [36], it is easy to verify that $\Theta_1 \geq 0$, $\Theta_2 \geq 0$, and $\Theta_3 \geq 0$. Using this observation in (52), it is easy to verify that

$$\triangle_i^* - d_i^* \geq 0 \ \text{ if } \alpha_i \leq \frac{e_{1,i}}{\Theta_1} \ \text{ for } \Theta_1 > 0, \tag{53}$$

$$d_{i+1}^* - \triangle_i^* \geq 0 \ \text{ if } \ \alpha_i \leq \frac{f_{1,i}}{\Theta_2} \ \text{ for } \Theta_2 > 0, \tag{54}$$

$$d_{i+1}^* - d_i^* \geq 0 \ \text{ if } \ \alpha_i \leq \frac{h_{1,i}}{\Theta_3} \ \text{ for } \Theta_3 > 0. \tag{55}$$

$$\text{If } \Theta_1 = 0, \Theta_2 = 0, \text{ and } \Theta_3 = 0, \text{ then } \triangle_i^* - d_i^* \geq 0, \ d_{i+1}^* - \triangle_i^* \geq 0, \text{ and } d_{i+1}^* - d_i^* \geq 0, \text{ respectively.} \tag{56}$$

Therefore from (53)–(56), we conclude that $\triangle_i^* - d_i^* \geq 0$, $d_{i+1}^* - \triangle_i^* \geq 0$, $d_{i+1}^* - d_i^* \geq 0$, and Ψ'' exists on $[x_1, x_n]$ if the scaling factors are chosen according to (47). Including (47), the sufficient conditions for $A_{1,i}^* \geq 0$, and $A_{8,i}^* \geq 0$ are

$$\left.\begin{array}{l} v_i = w_i, \\ v_i(\triangle_i^* - d_i^*) - (d_{i+1}^* - d_i^*) \geq 0, \\ w_i(d_{i+1}^* - \triangle_i^*) - (d_{i+1}^* - d_i^*) \geq 0. \end{array}\right\} \tag{57}$$

Now it is easy to see that (57) is equivalent to (48). If $\triangle_i - d_i = 0$ or $d_{i+1} - \triangle_i = 0$, (57) is true whenever $\alpha_i = 0$, $d_i = d_{i+1} = \triangle_i$. In this case, Ψ will be an affine map in $[x_i, x_{i+1}]$, i.e.,

$$\Psi(L_i(x)) = (1 - \theta) f_i + \theta f_{i+1}, \ \text{ and in this case } \Psi \text{ is convex over } [x_i, x_{i+1}].$$

After some simplification, it is found that the conditions (47) and (48) are sufficient for $A_{j,i}^* \geq 0$, for all $j = 2, \ldots, 7$. Thus, the conditions (47) and (48) are sufficient to obtain a convexity preserving rational cubic FIF Ψ for a given convex data. The uniqueness of a convex rational cubic FIF for a fixed set of parameters follows from the fixed point theorem.

Proceeding with a concave data set, we can show that the conditions (47) and (48) are sufficient to obtain a concavity preserving rational cubic FIF Ψ, and the theorem is proved.

Remark 4 If $\alpha_i = 0, i = 1, 2, \ldots, n-1$, then the conditions on the shape parameters v_i and $w_i, i = 1, 2, \ldots, n-1$, in the description of shape preserving aspect of the rational cubic FIF Ψ coincide with the corresponding shape preserving conditions of the classical rational cubic interpolant [31].

5 Illustration of shape preserving results

5.1 Examples and discussion of monotonic rational FIFs

Consider the monotonically increasing Akima data {(0, 10), (2, 10), (3, 10), (5, 10), (6, 10), (8, 10), (9, 10.5), (11, 15), (12, 50), (14, 60), (15, 85)} [1].

Using the rational IFS (17), we have constructed all our monotonicity preserving rational cubic FIFs, where the derivative values are approximated by the Arithmetic Mean Method only. We take $n = 11$ in the IFS (17) for the given Akima data. Since $\triangle_i = 0$ for $i = 1, 2, \ldots, 5$, take $\alpha_i = 0$ for $i = 1, 2, \ldots, 5$, and calculations of the shape parameters v_i and $w_i, i = 1, 2, \ldots, 5$ using (35) or (36) are not required. Since $d_6 = d_1 = 0$, we have $d_6^* = 0$. Therefore, for the sub-interval $[x_6, x_7]$, $\triangle_6^* - \frac{d_6^*}{v_6} \geq 0$ (see 35) is automatically true for any $v_6 \neq 0$. Due to this reason, we have taken $v_6 = 1$ in the construction of the rational cubic FIFs in Fig. 2a–h. To preserve the monotonic nature of Akima data, the scaling factors ($\alpha_i, i = 6, 7, \ldots, 10$) and shape parameters ($v_i, w_i, i = 7, \ldots, 10, w_6$) are chosen according to (34) and either (35) or (36), respectively. From (34), it is clear that the scaling factors depend on both interpolation data and corresponding derivatives. Therefore for Akima data, the scaling factors are restricted as $\alpha_6 \in [0, 0.0023]$, $\alpha_7 \in [0, 0.06]$, $\alpha_8 \in [0, 0.0526]$, $\alpha_9 \in [0, 0.0772]$, $\alpha_{10} \in [0, 0.0667)$ using (34). Also from (35) or (36), it is clear that the shape parameters depend on the given interpolation data, corresponding derivatives and scaling factors. Hence for different choices of the scaling vectors, we can restrict the shape parameters in various ways. Also for a fixed set of scaling factors, we can restrict the shape parameters v_i and w_i in different ways by choosing $l_i, k_i \in \mathbb{R}^+$ such that $\frac{1}{l_i} + \frac{1}{k_i} \leq 1$ according to (35). Choice of the scaling vectors and shape parameters in the construction of the $\mathcal{C}^1$-rational cubic FIFs (see Fig. 2a–j) are displayed in Table 1. In the construction of Fig. 2a–h, the shape parameters are chosen according to (35).

A reference $\mathcal{C}^1$-rational cubic FIF is generated in Fig. 2a with the suitably chosen scaling factors (see Table 1). Then the scaling factor α_7 is changed as 0.001 with respect to the IFS parameters of Fig. 2a, and the corresponding rational cubic FIF is constructed (see Fig. 2b). By analyzing Fig. 2b with respect to Fig. 2a, we have found visually pleasing changes in $[x_7, x_8]$, and there is no change in other sub-intervals. In particular, lower value of α_7 improves smoothness of the graph in the seventh sub-interval. Bold numerics in Table 1 represents the modified IFS parameters of Fig. 2a. Similarly by changing α_9 (see Table 1) with respect to the IFS parameters of Fig. 2a, the rational cubic FIF is constructed in Fig. 2c. By careful examination of Fig. 2c with Fig. 2a, it is observed that as $\alpha_9 \to 0^+$, a part of the rational cubic FIF corresponding to the ninth sub-interval is smoothened to a convex curve. Next Fig. 2d–f are generated by modifying either w_7 or v_8 or v_{10}, respectively with respect to the

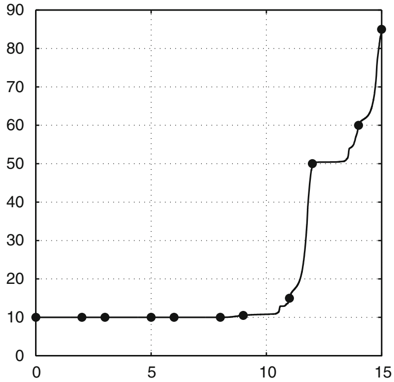

(a) A Reference rational cubic FIF.

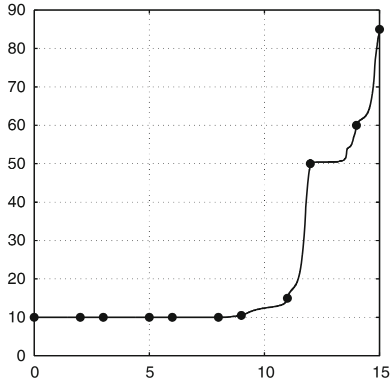

(b) Effects of α_7 in Fig. 2(a).

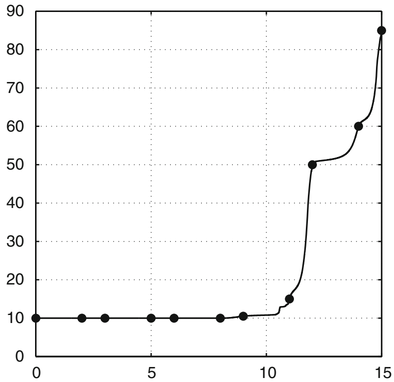

(c) Effects of α_9 in Fig. 2(a).

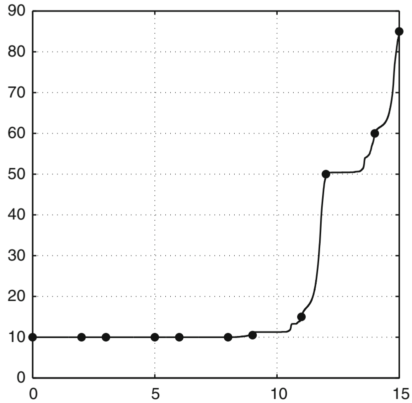

(d) Effects of w_7 in Fig. 2(a).

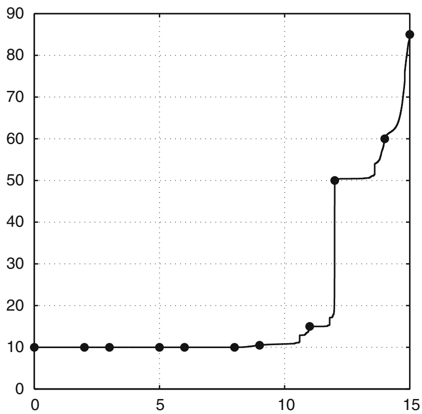

(e) Effects of v_8 in Fig. 2(a).

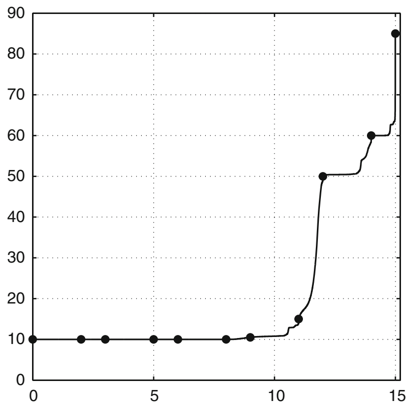

(f) Effects of v_{10} in Fig. 2(a).

Fig. 2 Monotonicity preserving rational cubic FIFs

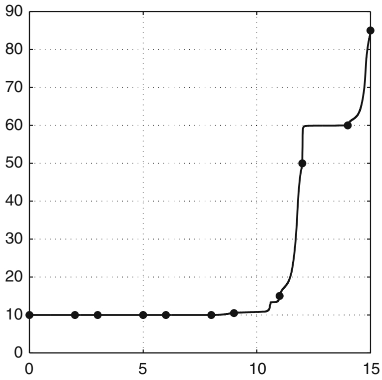

(g) Effects of w_9 in Fig. 2(c).

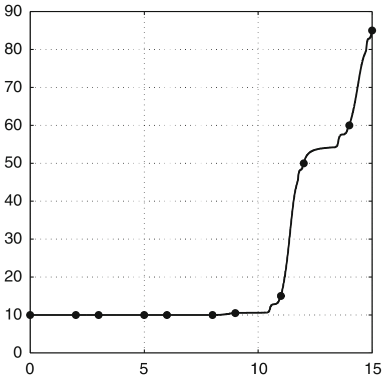

(h) Use of the condition (36).

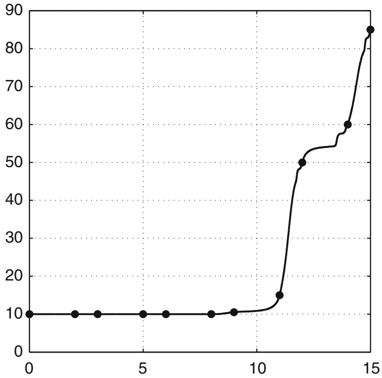

(i) Effects of α_7 in Fig. 2(h) using (36).

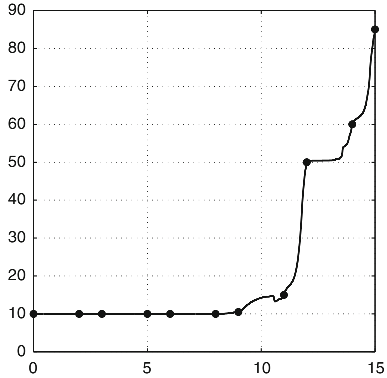

(j) Non-monotonic rational cubic FIF.

Fig. 2 continued

rational IFS parameters of Fig. 2a (see Table 1). An examination of Fig. 2d with respect to Fig. 2a reveals that the rational cubic FIF in the seventh sub-interval in Fig. 2d shifted above without altering any major changes. In comparison with Fig. 2b, we conclude that the scaling factor α_7 dominates the shape of rational FIF over the shape parameters v_7 and w_7 for Akima data. Above illustrations reveal that effects in the rational cubic FIF with respect to the changes in the scaling factors α_7, α_9 and shape parameter w_7 are very much local in nature. Next by comparing Fig. 2e with respect to Fig. 2a, we observe discernible changes in the seventh and eighth sub-intervals in Fig. 2e. It is easy to detect visually pleasing changes in the ninth and tenth sub-intervals in Fig. 2f in comparison with Fig. 2a. Similarly, the rational cubic FIF in Fig. 2g is produced by modifying only w_9 with respect to the IFS parameters of Fig. 2c (see Table 1). Due to a change in the shape parameter w_9, the convex shape of the rational cubic FIF in the ninth sub-interval in Fig. 2c is transformed as union of two straight lines in Fig. 2g. From last three observations, we conclude that effects in the rational cubic FIF with respect to the changes in the shape parameters v_8, v_{10} and w_9 are moderately local in nature. The visually pleasing fractal curve

Fig. 2h is generated with the same scaling vector as in Fig. 2a, and shape parameters with respect to (36). Now, only α_7 changed as 0.001 with respect to the IFS parameters of Fig. 2h, and the corresponding rational cubic FIF generated in Fig. 2i. By comparing Fig. 2i with respect to Fig. 2h, it is found that visually pleasing changes in the seventh sub-interval, and changes in other sub-intervals are negligible. Figure 2j explains the reason for the assumption that the scaling factors are to be non-negative, i.e., although we have chosen the shape parameters properly, since α_7 is negative (see Table 1), the rational cubic FIF in Fig. 2j is not monotonically increasing in the seventh sub-interval.

Table 1 Scaling factors and shape parameters used in the construction of monotonic rational cubic FIFs

Figure	Scaling factors	Shape parameters
2a	$\alpha_6 = 0.0021, \alpha_7 = 0.05, \alpha_8 = 0.0525, \alpha_9 = 0.077, \alpha_{10} = 0.0665$	$v_7 = 28.8880, v_8 = 7.7532, v_9 = 118.3432, v_{10} = 9.1608, w_6 = 0.5010, w_7 = 65.1109, w_8 = 0.004, w_9 = 0.0431, w_{10} = 0.0079$
2b	$\alpha_6 = 0.0021, \alpha_7 = \mathbf{0.001}, \alpha_8 = 0.0525, \alpha_9 = 0.077, \alpha_{10} = 0.0665$	$v_7 = \mathbf{4.8963}, v_8 = 7.7532, v_9 = 118.3432, v_{10} = 9.1608, w_6 = 0.5010, w_7 = \mathbf{21.5555}, w_8 = 0.004, w_9 = 0.0431, w_{10} = 0.0079$
2c	$\alpha_6 = 0.0021, \alpha_7 = 0.05, \alpha_8 = 0.0525, \alpha_9 = \mathbf{0.001}, \alpha_{10} = 0.0665$	$v_7 = 28.8880, v_8 = 7.7532, v_9 = \mathbf{50.3778}, v_{10} = 9.1608, w_6 = 0.5010, w_7 = 65.1109, w_8 = 0.004, w_9 = \mathbf{7.2929}, w_{10} = 0.0079$
2d	$\alpha_6 = 0.0021, \alpha_7 = 0.05, \alpha_8 = 0.0525, \alpha_9 = 0.077, \alpha_{10} = 0.0665$	$v_7 = 28.8880, v_8 = 7.7532, v_9 = 118.3432, v_{10} = 9.1608, w_6 = 0.5010, w_7 = \mathbf{651{,}109}, w_8 = 0.004, w_9 = 0.0431, w_{10} = 0.0079$
2e	$\alpha_6 = 0.0021, \alpha_7 = 0.05, \alpha_8 = 0.0525, \alpha_9 = 0.077, \alpha_{10} = 0.0665$	$v_7 = 28.8880, v_8 = \mathbf{77{,}532}, v_9 = 118.3432, v_{10} = 9.1608, w_6 = 0.5010, w_7 = 65.1109, w_8 = 0.004, w_9 = 0.0431, w_{10} = 0.0079$
2f	$\alpha_6 = 0.0021, \alpha_7 = 0.05, \alpha_8 = 0.0525, \alpha_9 = 0.077, \alpha_{10} = 0.0665$	$v_7 = 28.8880, v_8 = 7.7532, v_9 = 118.3432, v_{10} = \mathbf{91{,}608}, w_6 = 0.5010, w_7 = 65.1109, w_8 = 0.004, w_9 = 0.0431, w_{10} = 0.0079$
2g	$\alpha_6 = 0.0021, \alpha_7 = 0.05, \alpha_8 = 0.0525, \alpha_9 = \mathbf{0.001}, \alpha_{10} = 0.0665$	$v_7 = 28.8880, v_8 = 7.7532, v_9 = \mathbf{50.3778}, v_{10} = 9.1608, w_6 = 0.5010, w_7 = 65.1109, w_8 = 0.004, w_9 = \mathbf{72{,}929}, w_{10} = 0.0079$
2h	$\alpha_6 = 0.0021, \alpha_7 = -0.5, \alpha_8 = 0.0525, \alpha_9 = 0.077, \alpha_{10} = 0.0665$	$v_7 = 0.5159, v_8 = 7.7532, v_9 = 118.3432, v_{10} = 9.1608, w_6 = 0.501, w_7 = 13.6032, w_8 = 0.004, w_9 = 0.0431, w_{10} = 0.0079$
2i	$\alpha_6 = 0.0021, \alpha_7 = 0.05, \alpha_8 = 0.0525, \alpha_9 = 0.077, \alpha_{10} = 0.0665$	$v_6 = w_6 = 0.2505, v_7 = w_7 = 35.4442, v_8 = w_8 = 0.7773, v_9 = w_9 = 11.8558, v_{10} = w_{10} = 0.92$
2j	$\alpha_6 = 0.0021, \alpha_7 = \mathbf{0.001}, \alpha_8 = 0.0525, \alpha_9 = 0.077, \alpha_{10} = 0.0665$	$v_6 = w_6 = 0.2505, v_7 = w_7 = \mathbf{11.2674}, v_8 = w_8 = 0.7773, v_9 = w_9 = 11.8558, v_{10} = w_{10} = 0.92$

5.2 Examples and discussion of positive rational FIFs

We construct different $\mathcal{C}^1$-positive rational cubic fractal interpolants iteratively for a random positive data set $\{(0, 0.5), (2, 1.5), (3, 7), (9, 9), (11, 13)\}$ using IFS (17) with $n = 5$. Since in the IFS, the derivative values d_i $(i = 1, 2, \ldots, 5)$ are unknowns, they are approximated by the Arithmetic Mean Method (see Sect. 3.2). In order to carry the positive nature of above positive data by a rational cubic FIF, the scaling factors $(\alpha_i, i = 1, 2, \ldots, 4)$ and shape parameters $(v_i, w_i, i = 1, 2, \ldots, 4)$ are chosen with respect to (42) and (43), respectively. From (42), it is clear that the choice of scaling factors depends only on the given positive data. In order to preserve the positivity of above positive data, the restrictions of the scaling factors according to (42) are given by $\alpha_1 \in [0, 0.115)$, $\alpha_2 \in [0, 0.0909)$, $\alpha_3 \in [0, 0.5455)$, $\alpha_4 \in [0, 0.1818)$. From (43), it is clear that, the shape parameters of a rational cubic FIF depend on the given data and corresponding scaling factors. Therefore, each fixed set of the scaling factors gives a new restriction to the shape parameters. Numerical values of the scaling factors and shape parameters used in the construction of $\mathcal{C}^1$-rational cubic FIFs (Fig. 3a–h) are displayed in Table 2. If a user is not satisfied with a positive rational cubic FIF, then the user can opt for a desired positive rational cubic FIF by playing with the scaling factors (within the restricted interval).

A standard rational cubic positive FIF in Fig. 3a is constructed with suitably chosen scaling factors (see Table 2). Figure 3b is generated by modifying the scaling factor α_1 as 0.01 with respect to the other IFS parameters of Fig. 3a. Careful examination of Fig. 3b with Fig. 3a confirms that the graph of the rational cubic FIF corresponding to $[x_1, x_2]$ is convex whereas the graph of cubic FIF in the first sub-interval in Fig. 3a is neither convex nor concave. Bold numerics in Table 2 represents the modified IFS parameters of Fig. 3a. Figure 3c, d are constructed by changing the scaling factors α_3 and α_4 as 0.01 with respect to other IFS parameters of Fig. 3a (see Table 2), respectively. By analyzing Fig. 3c with respect to Fig. 3a, we observe visually pleasing changes in all sub-intervals of the graph. Similarly, by comparing Fig. 3d with respect to Fig. 3a, perceptible effects in the third and fourth sub-intervals are found. In particular as $\alpha_4 \to 0^+$, the graph of the rational cubic FIF corresponding to the fourth sub-interval in Fig. 3d is converging to a straight line. Next the $\mathcal{C}^1$-rational cubic FIFs in Fig. 3e, f are generated by modifying only v_1 or w_2, respectively, with respect to Fig. 3a. By comparing Fig. 3e with respect to Fig. 3a, we have found perceptible effects in the first and third sub-intervals. Next an examination of Fig. 3f with respect to Fig. 3a reveals palpable effects in all sub-intervals. Thus we have experimentally observed that assigning large values to v_1 or w_2 with respect to the IFS parameters of Fig. 3a yield similar types of rational cubic FIFs as in Fig. 3e, f, but with large deviations in the respective intervals. Similarly, Fig. 3g is constructed by modifying the shape parameter v_4 with respect to Fig. 3d. In comparison of Fig. 3g with respect to Fig. 3a, we observe visually pleasing changes in all sub-intervals even if v_4 modified alone. Again analyzing Fig. 3a, d, g, it is found that to obtain a straight line or convex shape at $[x_4, x_5]$ in Fig. 3a, one has to alter the scaling factor α_4 or/and shape parameter v_4 suitably. By using above discussion, it is easy to say that effects due to modification of the scaling factors α_1, α_4 and shape parameter v_1 are moderately local, whereas effects due to change in the scaling factor α_3 and shape parameters w_2 and v_4 are global for

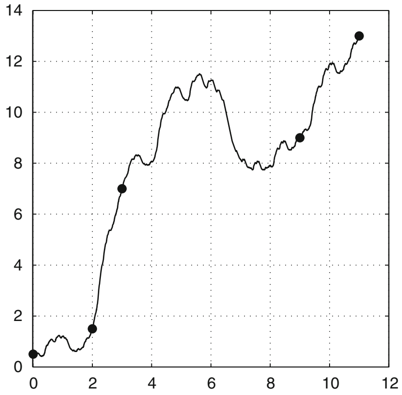

(a) A standard rational cubic positive FIF.

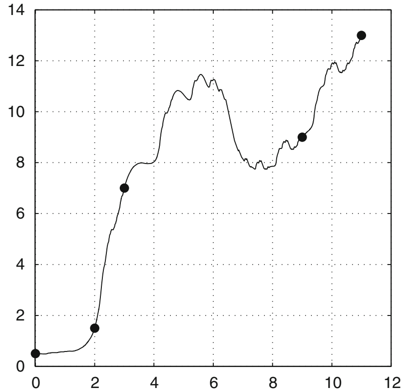

(b) Effects of α_1 in Fig. 3(a).

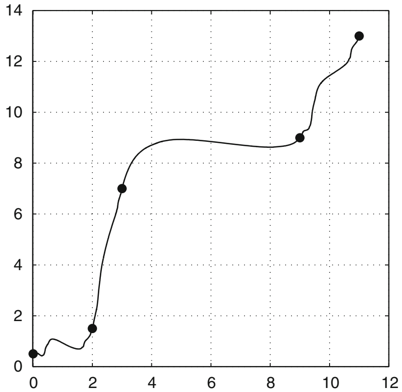

(c) Effects of α_3 in Fig. 3(a).

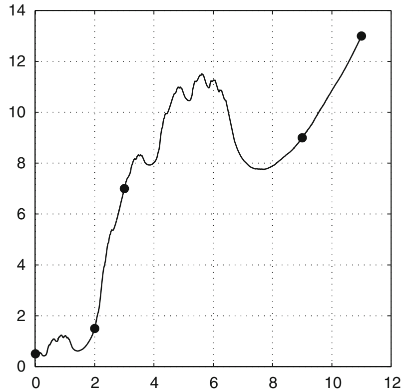

(d) Effects of α_4 in Fig. 3(a).

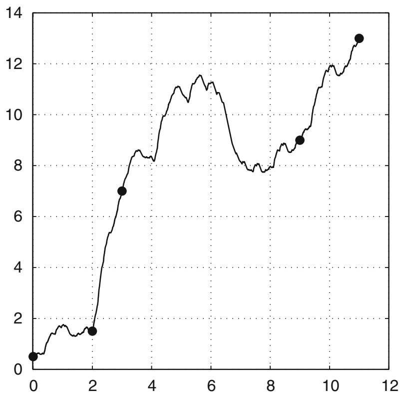

(e) Effects of v_1 in Fig. 3(a).

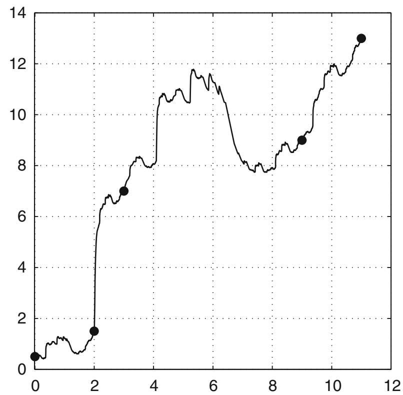

(f) Effects of w_2 in Fig. 3(a).

Fig. 3 Positivity preserving rational cubic FIFs

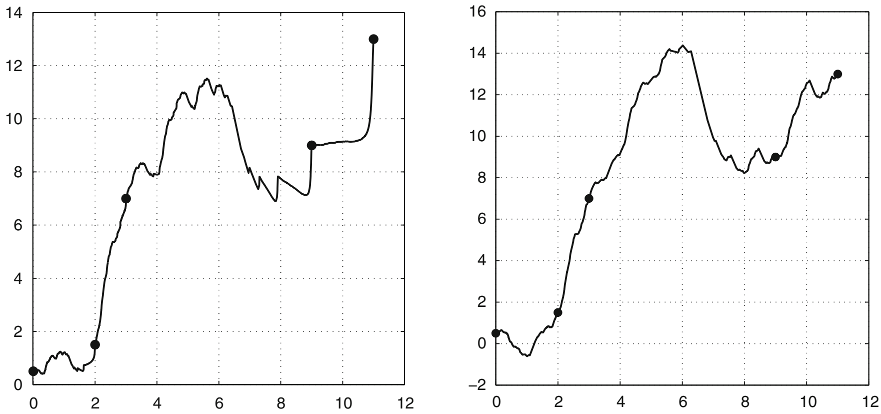

(g) Effects of v_4 in Fig. 3(d). **(h)** Non-positive rational cubic FIF.

Fig. 3 continued

Table 2 Scaling factors used in the construction of positive rational cubic FIFs

Figure	Scaling factors	Shape parameters
3a	$\alpha_1 = 0.115, \alpha_2 = 0.0908,$	$v_1 = 6, v_2 = 7.5, v_3 = 11, v_4 = 14,$
	$\alpha_3 = 0.545, \alpha_4 = 0.1815$	$w_1 = 7, w_2 = 11, w_3 = 16, w_4 = 12$
3b	$\alpha_1 = \mathbf{0.01}, \alpha_2 = 0.0908,$	$v_1 = 6, v_2 = 7.5, v_3 = 11, v_4 = 14,$
	$\alpha_3 = 0.545, \alpha_4 = 0.1815$	$w_1 = 7, w_2 = 11, w_3 = 16, w_4 = 12$
3c	$\alpha_1 = 0.115, \alpha_2 = 0.0908,$	$v_1 = 6, v_2 = 7.5, v_3 = 11, v_4 = 14,$
	$\alpha_3 = \mathbf{0.01}, \alpha_4 = 0.1815$	$w_1 = 7, w_2 = 11, w_3 = 16, w_4 = 12$
3d	$\alpha_1 = 0.115, \alpha_2 = 0.0908,$	$v_1 = 6, v_2 = 7.5, v_3 = 11, v_4 = 14,$
	$\alpha_3 = 0.545, \alpha_4 = \mathbf{0.01}$	$w_1 = 7, w_2 = 11, w_3 = 16, w_4 = 12$
3e	$\alpha_1 = 0.115, \alpha_2 = 0.0908,$	$v_1 = \mathbf{600}, v_2 = 7.5, v_3 = 11, v_4 = 14,$
	$\alpha_3 = 0.545, \alpha_4 = 0.1815$	$w_1 = 7, w_2 = 11, w_3 = 16, w_4 = 12$
3f	$\alpha_1 = 0.115, \alpha_2 = 0.0908,$	$v_1 = 6, v_2 = 7.5, v_3 = 11, v_4 = 14,$
	$\alpha_3 = 0.545, \alpha_4 = 0.1815$	$w_1 = 7, w_2 = \mathbf{1,100}, w_3 = 16, w_4 = 12$
3g	$\alpha_1 = 0.115, \alpha_2 = 0.0908,$	$v_1 = 6, v_2 = 7.5, v_3 = 11, v_4 = \mathbf{1,400},$
	$\alpha_3 = 0.545, \alpha_4 = \mathbf{0.01}$	$w_1 = 7, w_2 = 11, w_3 = 16, w_4 = 12$
3h	$\alpha_1 = -0.115, \alpha_2 = 0.0908,$	$v_1 = v_2 = v_3 = v_4 = 6,$
	$\alpha_3 = 0.545, \alpha_4 = 0.1815$	$w_1 = w_2 = w_3 = w_4 = 6$

this data. Also for the sub-interval $[x_i, x_{i+1}]$, $i = 1, 2, 3, 4,$ we have noticed that a modification of v_i or w_i impacts the rational cubic FIF in $[x_i, x_{i+1}]$ from the left-side or right-side, respectively. Since the selection of α_1 (see Table 2) is not followed according to (42), a part of the rational cubic FIF in Fig. 3h related to the first sub-interval is lying in the fourth quadrant. Hence, the positivity of the rational cubic FIF is lost in this case. Similarly, sufficiency of (42) can be proved with a suitable choice of the negative scaling factors and appropriate shape parameters for a positivity preserving rational cubic FIF.

5.3 Examples and discussion of convex rational FIFs

We construct different $\mathcal{C}^1$-convex rational cubic fractal interpolants iteratively for a convex data set $\{(0, 0), (0.5, 8.7713), (0.75, 18.8599), (1, 32.4673)\}$. These rational FIFs are attractors of IFS (17) with $n = 4$. This data was taken from a function which is twice differentiable, but its second derivative is non-negative, continuous and nowhere differentiable function. The derivative values d_i $(i = 1, 2, 3, 4)$ are approximated by the Arithmetic Mean Method (cf. Sect. 3.2). In the convexity preserving problems, the scaling factors depend on both interpolation data and corresponding derivatives according to (47). For the above convex data, the scaling factors are restricted as $\alpha_1 \in [0, 0.25), \alpha_2 \in [0, 0.0607), \alpha_3 \in [0, 0.0584)$ in our $\mathcal{C}^1$- rational cubic FIFs. Different choices of the scaling factors and shape parameters used in the generation of rational cubic FIFs (Fig. 4a–e) are given in Table 3.

The classical rational cubic interpolant Fig. 4a is generated by taking zero scaling vector. Changing v_1 and w_1 or v_2 or w_2 simultaneously with respect to the IFS parameters of Fig. 4a, we have observed graphically that there is no change in the shape of the classical rational FIF Fig. 4a. From these observations, we conclude that the classical rational cubic interpolant may not be too sensitive to the shape parameters for this convex data. Therefore, we wish to check the advantage obtained by our construction due to presence of the scaling factors. Now, we only modify the scaling factor α_1 as 0.23 (see Table 3), and the corresponding rational cubic FIF is generated in Fig. 4b. Bold numerics in Table 3 represents the modified IFS parameters of Fig. 4a. In comparison with Fig. 4a, we have observed perceptible effects in the rational cubic FIF in the first sub-interval and minor changes in other sub-intervals. It is found that all scaling factors are very much local in nature for this data. Similarly, the rational cubic FIF (see Fig. 4c) is generated by modifying α_2 and α_3 with respect to IFS parameters of Fig. 4a. In comparison with Fig. 4a, we have found visually pleasing effects in the second and third sub-intervals. Now modifications of the shape parameters $v_1 = w_1 = 200$ with respect to the IFS parameters of Fig. 4b yield Fig. 4d. By analyzing with Fig. 4b, we have noticed discernible effects in the first sub-interval. By comparing Fig. 4a, b, d, it is observed that for an aesthetic modification in the first sub-interval of Fig. 4a, we have to modify the scaling factor α_1 or/and shape parameters v_1, w_1 suitably. Figure 4e is developed with the negative scaling factors (see Table 3), and from this we conclude that our conditions (47) on the scaling factors for convexity are sufficient but not necessary. Figure 4f explains the importance of (47) in acquiring convexity preserving cubic rational FIFs for convex data, i.e., since $\alpha_i,\ i = 1, 2, 3,$ are chosen out of the above constrained intervals determined by (47), we lost the convexity feature in Fig. 4f.

6 Conclusion

Based on the calculus of rational FIFs, we have developed the $\mathcal{C}^1$-rational cubic FIFs that contain two families of shape parameters. With a zero scaling vector, the developed rational cubic FIF reduces to the existing classical rational cubic interpolant with two families of shape parameters. A uniform error bound has been developed between

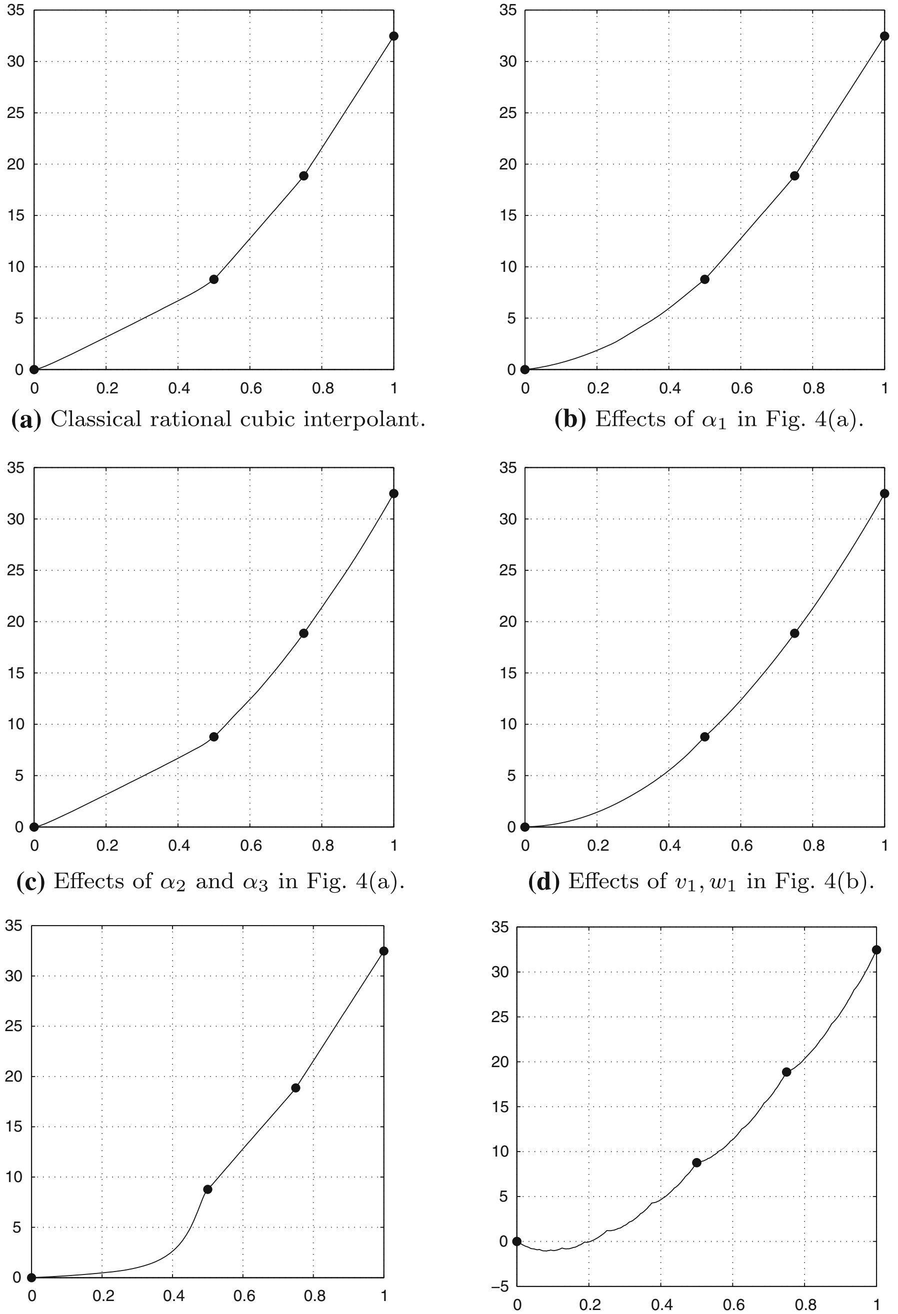

(a) Classical rational cubic interpolant.

(b) Effects of α_1 in Fig. 4(a).

(c) Effects of α_2 and α_3 in Fig. 4(a).

(d) Effects of v_1, w_1 in Fig. 4(b).

(e) Rational FIF with negative scaling factors.

(f) Non-convex rational cubic FIF.

Fig. 4 Convexity preserving rational cubic FIFs

Table 3 Scaling factors and shape parameters used in the construction of convex rational cubic FIFs

Figure	Scaling factors	Shape parameters
4a	$\alpha_1 = \alpha_2 = \alpha_3 = 0$	$v_1 = w_1 = 20, v_2 = w_2 = 30, v_3 = w_3 = 100$
4b	$\alpha_1 = \mathbf{0.23}, \alpha_2 = \alpha_3 = 0$	$v_1 = w_1 = 20, v_2 = w_2 = 30, v_3 = w_3 = 100$
4c	$\alpha_1 = 0, \alpha_2 = \mathbf{0.0605}, \alpha_3 = \mathbf{0.0581}$	$v_1 = w_1 = 20, v_2 = w_2 = 30, v_3 = w_3 = 100$
4d	$\alpha_1 = \mathbf{0.23}, \alpha_2 = \alpha_3 = 0$	$v_1 = w_1 = \mathbf{200}, v_2 = w_2 = 30, v_3 = w_3 = 100$
4e	$\alpha_1 = -0.01, \alpha_2 = -0.00605, \alpha_3 = -0.0001$	$v_1 = w_1 = 20, v_2 = w_2 = 30, v_3 = w_3 = 100$
4f	$\alpha_1 = 0.45, \alpha_2 = 0.2, \alpha_3 = 0.2$	$v_1 = w_1 = 20, v_2 = w_2 = 30, v_3 = w_3 = 100$

the rational cubic FIF and an original function. It is found that the developed rational cubic FIF converges uniformly to the original function. If we take $|\alpha_i| < a_i^2$, then it is possible to get quadratic convergence in our construction. The rational IFS scheme is either local or moderately local or global depending on the magnitude of the scaling factors and shape parameters. Simple constraints are made on free parameters, namely, the scaling factors and shape parameters in the description of the rational cubic FIF to visualize monotonic, positive, and convex data through the monotonic, positive, and convex fractal curves, respectively. The advantage of the developed rational cubic FIF over the existing interpolants are: (i) no extra knots are inserted to preserve the monotonicity of monotonic data (ii) no derivative constraints are imposed [14]. So, the developed rational cubic FIF is equally applicable to both data and data with slopes at the knots. Using possible choices of the scaling factors and shape parameters, pleasantness of graphical display, and the power of the proposed rational cubic FIF have been demonstrated through suitable examples. Software based on the developed scheme is under progress.

Acknowledgments The partial support of the Department of Science and Technology of Govt. of India (SERC DST Project No. SR/S4/MS: 694/10) is gratefully acknowledged. The authors are thankful to the referees for their valuable suggestions to improve the presentation of the article.

References

1. Akima, H.: A new method of interpolation and smooth curve fitting based on local procedures. J. Assoc. Comput. Mach. **17**, 589–602 (1970)
2. Barnsley, M.F.: Fractal functions and interpolation. Constr. Approx. **2**, 303–329 (1986)
3. Barnsley, M.F.: Fractals Everywhere. Academic Press, Orlando (1988)
4. Barnsley, M.F., Harrington, A.N.: The calculus of fractal interpolation functions. J. Approx. Theory. **57**, 14–34 (1989)
5. Beliakov, G.: Monotonicity preserving approximation of multivariate scattered data. BIT **45**(4), 653–677 (2005)
6. Chand, A.K.B., Kapoor, G.P.: Generalized cubic spline fractal interpolation functions. SIAM J. Numer. Anal. **44**(2), 655–676 (2006)
7. Chand, A.K.B., Navascués, M.A.: Generalized Hermite fractal interpolation. Rev. Real Acad. Cienc. Zaragoza **64**, 107–120 (2009)
8. Chand, A.K.B., Viswanathan, P.: Cubic Hermite and cubic spline fractal interpolation functions. In: AIP Conference Proceedings, vol. 1479, pp. 1467–1470 (2012)
9. Delbourgo, R., Gregory, J.A.: C^2 rational quadratic spline interpolation to monotonic data. IMA J. Numer. Anal. **3**, 141–152 (1983)

10. Delbourgo, R., Gregory, J.A.: Shape preserving piecewise rational interpolation. SIAM J. Sci. Stat. Comp. **6**(1), 967–976 (1985)
11. Dimri, V.P.: Applications of Fractals in Earth Sciences. A. A. Balkema Publishers, Brookfield (2000)
12. Duan, Q., Djidjeli, K., Price, W.G., Twizell, E.H.: The approximation properties of some rational cubic splines. J. Comp. Math. **72**, 155–166 (1999)
13. Feder, J.: Fractals (Physics of Solids and Liquids). Plenum Press, New York (1988)
14. Fritsch, F.N., Carlson, R.E.: Monotone piecewise cubic interpolation. SIAM J. Numer. Anal. **17**(2), 238–246 (1980)
15. Fritsch, F.N., Butland, J.: A method for constructing local monotone piecewise cubic interpolants. SIAM J. Sci. Stat. Comp. **5**, 303–304 (1984)
16. Fuhr, R.D., Kallay, M.: Monotone linear rational spline interpolation. CAGD **9**, 313–319 (1992)
17. Goodman, T.N.T., Unsworth, K.: Shape preserving interpolation by curvature continuous parametric curves. CAGD **5**, 323–340 (1988)
18. Gregory, J.A., Delbourgo, R.: Piecewise rational quadratic interpolation to monotonic data. IMA J. Numer. Anal. **2**, 123–130 (1982)
19. Gregory, J.A., Delbourgo, R.: Determination of derivative parameters for a monotonic rational quadratic interpolant. IMA J. Numer. Anal. **5**, 397–406 (1985)
20. Gregory, J.A., Sarfraz, M.: A rational spline with tension. CAGD **7**, 1–13 (1990)
21. Heck, A., Perdang, J.M.: Appl. Fractals Astron. Springer, Berlin (1991)
22. Hutchinson, J.E.: Fractals and self similarity. Indiana Univ. Math. J. **30**(5), 713–747 (1981)
23. Hutchinson, J., Lo, A., Poggio, T.: A nonparametric approach to pricing and hedging derivative securities via learning networks. J. Finance **49**, 851–889 (1994)
24. Kumar, V., Gavrilova, L., Tan, C.J.K., Ecuyer, P.L.: Computational science and its applications. In: ICCSA. Springer, Berlin (2003)
25. Lamberti, P., Manni, C.: Shape preserving C^2 functional interpolation via parametric curves. Numer. Algorithms **28**, 229–254 (2001)
26. Mandelbrot, B.: The Fractal Geometry of Nature. Freeman, San Francisco (1982)
27. Maragos, P.: Fractal aspects of speech signals: dimension and interpolation. ICASSP **1**, 417–420 (1991)
28. Navascués, M.A., Sebastián, M.V.: Smooth fractal interpolation. J. Inequalities Appl., 1–20. Article ID **78734** (2006)
29. Passow, E., Roulier, J.A.: Monotone and convex spline interpolation. SIAM J. Numer. Anal. **14**, 904–909 (1977)
30. Passow, E.: Monotone quadratic spline interpolation. J. Approx. Theory **19**, 143–147 (1977)
31. Sarfraz, M., Hussain, M.Z.: Data visualization using rational spline interpolation. J. Comp. Appl. Math. **189**, 513–525 (2006)
32. Sarfraz, M., Al-Mulhem, M., Ashraf, F.: Preserving monotonic shape of the data using piecewise rational cubic functions. Comput. Graph. **21**(1), 5–14 (1997)
33. Schmidt, J.W., HeB, W.: Positivity of cubic polynomial on intervals and positive spline interpolation. BIT **28**, 340–352 (1988)
34. Schumaker, L.L.: On shape preserving piecewise quadratic spline interpolation. SIAM J. Numer. Anal. **20**, 854–864 (1983)
35. Schweikert, D.G.: Interpolatory tension splines with automatic selection of tension factors. J. Math. Phys. **45**, 312–317 (1966)
36. Sohrab, H.H.: Basic Real Anal. Birkhäuser, Boston (2003)
37. Shrivastava, M., Joseph, J.: C^2-rational cubic spline involving tension parameters. Proc. Indian Acad. Sci. Math. Sci. **110**(3), 305–314 (2000)
38. Tian, M.: Monotonicity preserving piecewise rational cubic interpolation. Int. J. Math. Anal. **5**, 99–104 (2011)
39. Wittenbrink, C.M.: IFS fractal interpolation for 2D and 3D visualization. In: Proceedings of the IEEE Visualization Conference, pp. 77–84 (1995)
40. Xie, H.: Fractals in Rock Mechanics. A. A. Balkema Publishers, Brookfield (1993)
41. Zimmermann, H.J.: Fuzzy set theory and its applications. Kluwer, Boston (1996)